CCR2-dependent monocyte-derived macrophages resolve inflammation and restore gut motility in postoperative ileus

Gut

CCR2-dependent monocyte-derived macrophages resolve inflammation and restore gut motility in postoperative ileus.

Journal:	*Gut*
Manuscript ID	gutjnl-2016-313144.R1
Article Type:	Original Article
Date Submitted by the Author:	n/a
Complete List of Authors:	Farro, Giovanna; University of Leuven, Dept. Gastroenterology, Stakenborg, Michelle; University of Leuven, Dept. Gastroenterology, Gomez-Pinilla, Pedro J.; University of Leuven, Dept. Gastroenterology, Labeeuw, Evelien; University of Leuven, Dept. Gastroenterology, Goverse, Gera; University of Leuven, Dept. Gastroenterology, Di Giovangiulio, Martina; University of Leuven, Dept. Gastroenterology, Stakenborg, Nathalie; University of Leuven, Dept. Gastroenterology, Meroni, Elisa; University of Leuven, Dept. Gastroenterology, D'Errico, Francesca; University of Leuven, Dept. Gastroenterology, Elkrim, Yvon; Inflammatie-researchcentrum, Myeloid Cell Immunology Lab; Vrije Universiteit Brussel, VIB Lab of Myeloid Cell Immunology Laoui, Damya; Inflammatie-researchcentrum, Myeloid Cell Immunology Lab; Vrije Universiteit Brussel, Lab of Cellular and Molecular Immunology Lisowski, Zofia M.; University of Edinburgh Roslin Institute Sauter, Kirsten A.; University of Edinburgh Roslin Institute Hume, David; University of Edinburgh Roslin Institute Van Ginderachter, Jo; Inflammatie-researchcentrum, Myeloid Cell Immunology Lab; Vrije Universiteit Brussel, VIB Lab of Myeloid Cell Immunology Boeckxstaens, Guy; Catholic University of Leuven, Gastroenterology Matteoli, Gianluca; University of Leuven, Dept. Gastroenterology,
Keywords:	MACROPHAGES, INFLAMMATION, GASTROINTESTINAL TRANSIT

Title page:

CCR2-dependent monocyte-derived macrophages resolve inflammation and restore gut motility in postoperative ileus.

Short title: Macrophages resolve postoperative ileus

Giovanna Farro[1], Michelle Stakenborg[1], Pedro J Gomez-Pinilla[1], Evelien Labeeuw[1], Gera Goverse[1], Martina Di Giovangiulio[1], Nathalie Stakenborg[1], Elisa Meroni[1], Francesca D'Errico[1], Yvon Elkrim[2,3], Damya Laoui[2,3], Zofia M. Lisowski[4], Kristin A. Sauter[4], David A. Hume[4], Jo A. Van Ginderachter[2,3], Guy E. Boeckxstaens[1#] & Gianluca Matteoli[1#].

[1]KU Leuven Department of Clinical and Experimental Medicine, Translational Research Center for Gastrointestinal Disorders (TARGID), Leuven, Belgium. [2]Myeloid Cell Immunology Lab, VIB Inflammation Research Center, Ghent, Belgium. [3]Lab of Cellular and Molecular Immunology, Vrije Universiteit Brussel, Pleinlaan 2, B-1050 Brussels, Belgium. [4]The Roslin Institute and Royal (Dick) School of Veterinary Studies, University of Edinburgh, Easter Bush, EH25 9RG, UK.

[#] These authors contributed equally as co-last authors.

Corresponding authors:

Prof. Gianluca Matteoli & **Prof. Guy E. Boeckxstaens**
Department of Clinical and Experimental Medicine
Translational Research Center for Gastrointestinal Disorders (TARGID)
KU Leuven; Herestraat 49, O&N1, bus 701; 3000, Leuven, Belgium
Tel: +32-16-330238/ +32-16-345750

E-mail: **gianluca.matteoli@kuleuven.be** and **guy.boeckxstaens@kuleuven.be**

Word count: 4314

Summary 'box':

What is already known about this subject?

- Monocytes and neutrophils infiltrate the *muscularis externa* within a few hours after abdominal surgery
- Infiltration of neutrophils and monocytes after surgery has been correlated to impaired muscle contraction and delayed intestinal transit typical of postoperative ileus

What are the new findings?

- Blocking influx of monocyte migration to the *muscularis externa* after intestinal manipulation does not prevent postoperative ileus
- Lack of monocyte migration to the *muscularis externa* may have dramatic side effects on the recovery of GI transit after open abdominal surgery associated with increased neutrophil-mediated immunopathology and persistent impaired neuromuscular function
- Monocyte-derived macrophages are crucial to the resolution of muscularis inflammation and recovery of gastro-intestinal functions during postoperative ileus

How might it impact on clinical practice in the foreseeable future?

- Our findings imply that inappropriate targeting of the cellular immune response may increase neutrophil-mediated immunopathology and prolong the clinical outcome of POI
- Future therapies should be aimed at enhancing physiological repair functions of macrophages rather than preventing monocyte recruitment to the tissue.

Abstract

Objective. Postoperative ileus (POI) is assumed to result from myeloid cells infiltrating the intestinal *muscularis externa* (ME) in patients undergoing abdominal surgery. In the current study, we investigated the role of infiltrating monocytes in a murine model of intestinal manipulation (IM)-induced POI in order to clarify whether monocytes mediate tissue damage and intestinal dysfunction or they are rather involved in the recovery of intestinal motility. **Design**. IM was performed in mice with defective monocyte migration to tissues (C-C motif chemokine receptor 2, *Ccr2*$^{-/-}$ mice) and wild-type (WT) mice to study the role of monocytes and monocyte-derived macrophages (MΦs) during onset and resolution of ME inflammation. **Results.** At early time points, IM-induced GI transit delay and inflammation were equal in WT and *Ccr2*$^{-/-}$ mice. However, GI transit recovery after IM was significantly delayed in *Ccr2*$^{-/-}$ mice compared to WT mice, associated with increased neutrophil-mediated immunopathology and persistent impaired neuromuscular function. During recovery, monocytes differentiated into MΦs and up-regulated pro-resolving genes. Treatment with MΦ colony-stimulating factor 1 (CSF1) enhanced monocyte recruitment and MΦ differentiation and ameliorated GI transit in *Ccr2*$^{-/-}$ mice. **Conclusion.** Our study reveals a critical role for monocyte-derived MΦs in restoring intestinal homeostasis after surgical trauma. From a therapeutic point of view, our data indicate that inappropriate targeting of monocytes may increase neutrophil-mediated immunopathology and prolong the clinical outcome of POI, while future therapies should be aimed at enhancing MΦ physiological repair functions.

Key words: postoperative ileus; monocytes; monocyte-derived macrophages; colony-stimulating factor 1.

Introduction

Abdominal surgery is often associated with a transient episode of intestinal dysmotility accompanied by symptoms ranging from abdominal pain to constipation and the inability to tolerate a solid diet, referred to as postoperative ileus (POI) (1). Besides the discomfort experienced by patients and possible complications, POI is the most common cause of prolonged hospital stay following abdominal surgery and the annual cost has been estimated as much as $ 1.5 billion in USA, having a large socio-economic impact (2).

POI is a multifactorial condition deriving from many surgery-related factors that contribute to reduce the contractility of the intestinal *muscularis externa* (ME) and to delay GI transit after surgery. For example, the effect of anesthetics, postoperative opioids, inhibitory neural reflexes and inflammatory mediators released by immune cells invading the ME after surgical handling of the intestine have been shown to concur with the development of POI (1).

One of the earliest steps in the inflammatory cascade occurring after abdominal surgery is activation of ME resident macrophages (MΦs), a uniquely adapted population of resident MΦs (3;4). At steady state, ME MΦs respond to luminal bacterial infections and interact with enteric neurons to regulate gastrointestinal motility (5). Once activated, resident MΦs recruit leukocytes, in particular monocytes and neutrophils to the ME, within a few hours after surgery (6). Infiltration of neutrophils and monocytes after surgery has been temporally correlated with impaired muscle contraction and delayed intestinal transit (7). Previous studies have shown that inactivation or depletion of resident MΦs prior to surgery prevented leukocyte recruitment and ameliorated GI transit (7;8). A similar beneficial outcome was obtained by blocking adhesion molecules on the endothelial surface to prevent leukocyte infiltration (6;9;10). However, during inflammation recruitment of leukocytes, and in particular monocytes, is crucial to the timely resolution of the inflammatory process and to prevent excessive tissue damage. In the context of sterile inflammation, while $CCR2^+$ circulating monocytes may initiate pathology, monocyte-derived MΦs typically undergo alternative activation

and acquire a pro-resolving phenotype. Monocyte-derived MΦs have been shown to be critical for repair and functional recovery of various types of organs (11-13), via the release of anti-inflammatory and reparative cytokines and growth factors (14;15). In the context of POI, anti-inflammatory mediators such as the immune-modulatory cytokine IL-10 and poly-unsaturated fatty acids (PUFA)-derived pro-resolving molecules have been shown to be involved in the recovery of intestinal motility (16-18). However, mechanisms of inflammation and resolution have not been fully clarified and the role of monocyte trafficking the ME and MΦ function following surgery remains to be determined.

In the current study, using CCR2-deficient mice (*Ccr2*$^{-/-}$), we investigated the role of infiltrating monocytes in a murine model of IM-induced POI in order to clarify whether monocytes mediate tissue damage and intestinal dysfunction or are rather involved in the recovery of intestinal motility after surgical trauma. In contrast with the current view, our study demonstrates that CCR2-mediated monocyte infiltration does not contribute to the development of surgery-induced POI. Conversely, monocyte-derived MΦs acquire a pro-resolving phenotype and are essential for postoperative recovery. In line, treatment with colony-stimulating factor 1 (CSF1) could overcome CCR2 deficiency and promote monocyte migration to the ME accelerating resolution of inflammation and recovery of GI motility. Our work suggests that future therapies aiming at enhancing MΦ physiological repair functions may represent an ideal approach to accelerate recovery in patients with POI.

Material and Methods

Animals

Twelve week old female wild-type (WT; C57BL/6JOlaHsd), Ccr2 knockout (Ccr2$^{-/-}$; B6.129S4-*Ccr2*^{tm1Ifc}/J), and UBI-GFP (C57BL/6-Tg(UBC-GFP)30Scha/J) mice were kept at the KU Leuven animal facility under SPF conditions on a 12:12-h light-dark cycle and provided with commercially available chow (ssniff® R/M-H, ssniff Spezialdiäten GmbH) and tap water *ad libitum*. All experimental procedures were approved by the Animal Care and Animal Experiments Committee of the University of Leuven (Leuven, Belgium).

Experimental model of POI

An established model of intestinal manipulation (IM) was used to induce POI (19).. A midline laparotomy followed by IM was performed as previously reported (19). During and after the surgical procedure, mice were positioned on a heat pad (32°C) until they recovered from anesthesia. Naïve mice did not undergo any surgical procedure.

Statistical analysis

Significance between two groups was determined by unpaired two-tailed Student's t Test or non-parametric Mann-Whitney test, while one-way analysis of variance (one-way ANOVA) followed by Dunnett's Multiple comparison test was performed to compare multiple mean groups. Significance between dose/frequency-response curves was determined by two-way repeated ANOVA followed by Bonferroni post hoc analysis. Survival curves were compared via Gehan–Breslow-Wilcoxon Test. Graph Pad Prism V.5.01 software (GraphPad Software, Inc.) was used to generate graphs and perform statistical analysis.

Results

Surgical manipulation of the intestine induces early influx of leukocytes to the ME.

Consistent with previous studies (19), surgical manipulation of the intestine in WT mice led to a significant delay in GI transit (Fig. 1A), accompanied by a massive recruitment of immune cells into the ME during the 24 hours following IM (Fig. S1A). Upon intestinal handling, different immune cells accumulated into the ME with different recruitment patterns/dynamics (Fig. S1B). In line with typical models of sterile inflammation, neutrophils ($CD45^+CD11b^+Ly6G^+CD64^-$) were already detectable in the ME within 1 hour after surgery, peaking at 6 hours and representing 50% of the $CD45^+$ immune cell infiltrate at this time. Subsequently, major recruitment of monocytes/MΦs ($CD45^+CD11b^+Ly6G^-CD64^+$) occurred from 6 hours onwards, outnumbering neutrophils by more than 3-fold at 24 hours after IM (Fig. S1C).

Monocytes recruited to the ME after IM do not induce delay in GI transit.

The recruitment of classical CCR2-monocytes to the sites of tissue inflammation often mediates collateral tissue damage potentially inducing intestinal smooth muscle dysfunction typical of POI. To define the contribution of monocytes in the pathogenesis of POI, we performed IM in mice lacking the CCR2 receptor (*Ccr2*$^{-/-}$) showing defective trafficking of monocytes to the sites of inflammation (20). Of note, lack of CCR2 expression does not alter the typical ME resident MΦ population, with WT and *Ccr2*$^{-/-}$ mice showing similar distribution of $F4/80^+$ cells (Fig. S2A) and comparable number of $MHCII^{lo}$ $Ly6C^-$ MΦs and $MHCII^{hi}$ $Ly6C^-$ MΦs in the naïve ME (Fig. S2B). However, after IM CCR2-deficiency significantly prevented accumulation of monocytes in the ME of *Ccr2*$^{-/-}$ mice compared to WT mice (Fig. 1B). Nevertheless, 24 hours after IM *Ccr2*$^{-/-}$ mice showed delayed GI transit to the same extent as WT mice, excluding a direct effect of monocytes on the development of intestinal dysmotility (Fig. 1A). Moreover, *Ccr2*$^{-/-}$ mice showed similar expression of typical pro-inflammatory cytokines (*tnfa, il6* and *il1a)* and chemokines (*ccl2*, *cxcl1* and *cxcl2)* in the

ME as WT controls 24 hours after IM (Fig. 1C) with the exception of *il1b,* being significantly lower in *Ccr2*$^{-/-}$ mice. Thus, up-regulation of most pro-inflammatory cytokine encoding genes does not depend on monocytes. Taken together, our data indicate that monocytes, although massively recruited to the muscular tissue within 24 hours, are not essential for the initiation of POI.

Functional impairment of gastrointestinal motility in *Ccr2*$^{-/-}$ mice is associated with persistent neuronal impairment after IM.

Upon tissue damage or infection, monocytes are rapidly recruited to the tissue, where they differentiate into mature MΦs, playing an essential role in the resolution of inflammation and tissue repair. Thus, we reasoned that monocytes accumulating in the intestinal ME after IM could differentiate into MΦs being crucial for the resolution of inflammation and recovery. Interestingly, *in vivo* measurements of GI transit after the acute phase of POI (> 24 hours after IM) showed that GI transit delay was significantly prolonged in *Ccr2*$^{-/-}$ mice compared to WT counterparts (Fig. 2A). In detail, while in the WT mice the delay of GI transit mainly recovered 3 days after IM (with few mice recovering at day 5), normalization of GI transit in *Ccr2*$^{-/-}$ mice only started at day 5 with full recover only at day 10 after IM (Fig. 2A). Whereas all WT mice survived IM and recovered GI motility, 25% of *Ccr2*$^{-/-}$ mice failed to recover and died as consequence of prolonged ileus (Fig. 2B).

As GI transit delay in POI mainly depends on reduced functionality of the smooth muscle layer after IM, we determined if the prolonged transit delay observed in *Ccr2*$^{-/-}$ mice was caused by a more severe impairment in neuromuscular function. To this aim, contractility of smooth muscle strips isolated from the small bowel of WT and *Ccr2*$^{-/-}$ mice was recorded at different time points after IM (Fig. 2C-2E) using KCl and the muscarinic agonist carbachol (CCh) to evaluate respectively the Ca^{2+} sensitivity and the receptor-mediated contraction. In line with previous literature (21), IM significantly reduced both receptor-mediated and receptor-independent smooth muscle contractions in WT animals (Fig. S3 and S4). However, contractile responses were significantly smaller in intestinal muscle strips isolated from *Ccr2*$^{-/-}$ mice compared to WT mice 1 day after IM

(Fig. 2C-2D). At day 3 and 5 after IM, myogenic contractions to KCl and CCh were completely recovered both in WT and *Ccr2*$^{-/-}$ muscle strips (Fig. 2C-2D and S3-S4). Furthermore, considering the critical role played by enteric neurons in gastro-intestinal motility, we measured smooth muscle contractions evoked by electrical field stimulation (EFS) to evaluate the impact of IM on the function of enteric nervous system. EFS-induced contractions were reduced in manipulated WT and *Ccr2*$^{-/-}$ animals 1 day after surgery (Fig. S5A), but significantly more pronounced in *Ccr2*$^{-/-}$ mice (Fig. 2E). Contrarily to myogenic responses, EFS-induced contraction remained severely impaired in muscle strips isolated from *Ccr2*$^{-/-}$ mice for 5 days after IM (Fig. 2E and Fig. S5A). Of note, 30% of muscle strips isolated from *Ccr2*$^{-/-}$ mice 3 and 5 days after IM failed to contract to any stimuli suggesting severe alteration of neuromuscular function (data not shown). To evaluate impairment of enteric neurotransmission, EFS-induced contractions were normalized to the receptor-independent KCl-induced contraction of each muscle strip both in WT and *Ccr2*$^{-/-}$ mice at different time points after IM (Fig. S5B). Normalization showed that the "neural component" of EFS-evoked responses was significantly reduced in *Ccr2*$^{-/-}$ compared to WT mice at each time point measured demonstrating a severe dysfunction of enteric neurons after IM in the absence of monocyte recruitment to the ME (Fig. S5B).

In order to assess neural alteration at the morphological level, we used confocal microscopy to dissect the sub-cellular localization of HuC/D in enteric neurons in the myenteric plexus of WT and *Ccr2*$^{-/-}$ mice 5 days after IM (Fig. 3). Our data showed that HuC/D^{+} neurons are comparable in number, volume and neurotransmitters expression of choline acetyltransferase (ChAT) and nitric oxide synthase (nNOS) between the two groups (Fig. S6). However, we detected significantly higher nuclear localization of HuC/D^{+} in enteric neurons of *Ccr2*$^{-/-}$ mice (Fig. 3 and Fig. S7), suggestive of neuronal dysfunction (22;23). Overall, our data showed that neuromuscular function is severely affected in *Ccr2*$^{-/-}$ mice suggesting that monocytes protect neural function during ME inflammation.

Ccr2^{+} monocytes limit inflammation and neutrophil-mediated pathology after IM.

We hypothesized that impaired monocyte trafficking in *Ccr2*$^{-/-}$ mice prevented the switch of the inflammatory process towards resolution, which is orchestrated by monocyte-derived MΦs with regulatory and pro-resolving functions. In fact, local inflammation was prolonged in the ME of *Ccr2*$^{-/-}$ mice, as demonstrated by higher levels of pro-inflammatory cytokines until day 3 after IM (Fig. 4A), and only returning to basal levels at day 5 (data not shown). In addition, the ME of *Ccr2*$^{-/-}$ mice was populated with a higher number of activated neutrophils expressing reactive oxygen species (ROS) as well as IL-6 and TNFα when compared to WT mice (Fig. 4B). In keeping with the implied deregulation of the resolution process, *Ccr2*$^{-/-}$ mice showed increased tissue alterations, as thickening of the intestinal wall and increased deposition of collagen fibres at the level of the ME compared to WT controls (Fig. 4C-3E). Moreover, an increased number of intra-abdominal adhesions were detected 5 days after IM in *Ccr2*$^{-/-}$ mice compared to their WT counterparts (Fig. 4F). These data suggest that monocytes contribute to resolution of inflammation in part by modulating neutrophil influx to the injured ME.

MHCII^{+} monocyte-derived macrophages accumulate in the ME during recovery through CCR2-dependent and independent pathways.

Based upon the evidence that resolution of inflammation and recovery of dysmotility in POI depend on accumulation of monocyte-derived MΦs in the ME, we examined their phenotype and origin at steady state and after surgery in WT and *Ccr2*$^{-/-}$ mice. Of note, the muscularis resident MΦ populations (major population of MHCII^{hi} Ly6C^{-} MΦs and a smaller number of MHCII^{lo} Ly6C^{-} MΦs) of naïve WT and *Ccr2*$^{-/-}$ mice were indistinguishable in shape, number and location (Fig. S2). During the first 24 hours following surgery, neutrophils, classical Ly6C^{hi} monocytes, and Ly6C^{+}MHCII^{+} immature MΦs infiltrated the ME of WT mice (Fig. 5A-4D and Fig. S8). Three days after IM, Ly6C^{hi}MHCII^{-} monocytes were mostly differentiated into Ly6C^{-}MHCII^{lo} and Ly6C^{-}MHCII^{hi} MΦs in equal proportions (Fig. 5E and F). Five days after IM the number of mature MΦs returned to basal levels with a

predominance of MHCII^{hi} MΦs, resembling the steady state situation (Fig. 5A and C). As expected, the recruitment of Ly6C^{hi} monocytes was blunted in *Ccr2*$^{-/-}$ mice at day 1 after IM, associated with a marked reduction of immature and mature MΦs at the later time points compared to their WT counterparts (Fig. 5D-F and Fig. S8). Interestingly, only at day 5 the amount of MHCII^{lo} MΦs in *Ccr2*$^{-/-}$ was comparable to WT mice. This indicated that despite a certain delay, MΦs of the MHCII^{lo} subset can still accumulate in the ME and suggests the presence of CCR2-independent mechanisms of MΦ accumulation (Fig. 5 and Fig. S8).

In order to determine the relative importance of recruited monocytes differentiating *in situ* into MΦs, we first traced the differentiation process via adoptive transfer of Ly6C^{hi} monocytes isolated from UBI-GFP mice into WT mice prior to IM (Fig. 6). GFP^{+} cells were widely detected among the infiltrating monocytes and immature MΦs during the acute phase (day 1) and in both mature MΦ subsets throughout the resolution phase (day 3 and day 5, Fig. 6A and B). Secondly, we assessed the proliferation capacity of monocytes and MΦs in WT naïve ME via BrdU incorporation assay and Ki67 expression. Of note, MHCII^{hi} MΦs in naïve ME incorporated BrdU and expressed Ki67 showing a basal proliferation capacity even at steady state (Fig. 6C and D). After IM, monocytes and immature MΦs showed significant proliferation at day 1, while Ly6C^{-}MHCII^{lo} and Ly6C^{-}MHCII^{hi} MΦs expanded *in situ* mainly at day 3 (Fig. 6C-E). Taken together, these data indicate that MΦ accumulation after IM mainly depends on recruitment and expansion of circulating monocytes and to a minor extent, on the proliferation of resident MΦs. Thus, *Ccr2*$^{-/-}$ mice fail to mount an appropriate and self-limiting inflammatory response, leading to increased tissue damage and prolonged symptoms.

Macrophages acquire pro-resolving features during the recovery phase of POI.

To characterize pro-resolving MΦ features during the recovery phase of POI, we quantified expression levels of genes associated with classical or alternative MΦ activation states in *muscularis* tissue. Within the first few hours after IM (1,5 to 6 hours), pro-inflammatory cytokines *tnfa*, *il6*, *il1b* and *ccl2* were up-regulated (Fig. S9A), while 12 hours after IM typical IL-4-target genes such as *arg1*

and *ym1* were induced (Fig. S9B). Indeed, *il4* itself, which has been implicated in the control of MΦ proliferation during sterile inflammation was highly up-regulated in ME homogenates 12 hours after IM (Fig. S9B). In line, during the resolution phase (day 3 after IM), we detected a significant decrease of inflammatory genes such as *il1b* and an increase in gene expression levels of typical markers of alternative activated MΦs such as *mrc1, stab1* and *ym1* (Fig. 7A). To evaluate which cells express these genes, monocytes, MHCII^{lo} and MHCII^{hi} MΦs were sorted 3 days after IM and expression of pro-inflammatory and pro-resolving genes was evaluated. In detail, high expression of *il1b* and *nos2* were only detectable in monocytic cells, while being significantly lower in mature MΦs. On the contrary, *mrc1*, *arg1*, *stab1* and *ym1* were increased in MΦs compared to monocytes, indicating a differentiation towards a pro-resolving phenotype (Fig. 7B). Of note, expression of these anti-inflammatory markers was higher in the MHCII^{lo} subset (Fig. 7B). Overall, our data showed that MΦs are essential players in resolution of inflammation and restoration of tissue function in POI.

CSF1 drives pro-resolving macrophage differentiation and favours recovery of GI motility.

Based on the above, we hypothesized that favouring monocyte recruitment and their differentiation toward pro-resolving MΦs might represent a valuable therapeutic approach to accelerate recovery of GI function after IM. Thus, considering that the MΦ growth factor CSF1 promotes monocyte production, recruitment, maturation and local MΦ proliferation (24;25), we assessed the effect of CSF1-Fc administration in WT and *Ccr2*$^{-/-}$ mice during the recovery phase after IM (Fig. 8). As previously reported (26), CSF1-Fc treatment increased spleen (Fig. S10A) and liver weight (Fig. S10B) in WT and *Ccr2*$^{-/-}$ mice. Notably, CSF1-Fc treatment restored the accumulation of monocytes and increased MΦ differentiation into the ME of *Ccr2*$^{-/-}$ mice 3 days after IM (Fig. 8A and S11). Of note, CSF1-Fc treatment reduced neutrophil infiltration in the ME of WT and *Ccr2*$^{-/-}$ mice, indicating that monocytes and/or MΦs limited neutrophil entry (Fig. 8A). Consequently, CSF1-Fc-treated mice showed a significantly lower number of ROS-producing neutrophils (Fig. 8B). In addition, CFS1-Fc administration increased the expression of anti-inflammatory and pro-resolving

genes after IM (Fig. S12). Strikingly, with regard to intestinal motility, CSF1-treated *Ccr2*$^{-/-}$ mice recovered GI transit delay 3 days after IM to the same extent as WT mice (Fig. 8C). In line with the beneficial effect of CSF1, adoptive transfer of WT bone marrow into irradiated Ccr*2*$^{-/-}$ mice (WT→ *Ccr2*$^{-/-}$) also induced recovery of GI transit 3 days after IM, which did not differ from that of WT mice reconstituted with WT bone marrow (WT→ WT) (Fig. S13A). Moreover, we observed restored monocyte recruitment to the ME in WT→ *Ccr2*$^{-/-}$ and a significantly lower number of activated neutrophils when compared with non-reconstituted *Ccr2*$^{-/-}$ (Fig. S13 B-D).

Discussion

POI is a clinical condition of iatrogenic origin that occurs after abdominal surgery (1;27). Traditionally, postoperative inhibition of GI transit has been associated with inflammation of the ME and influx of leukocytes (6;9). Although the exact pathogenesis of POI is still not fully understood, prevention of inflammation-associated damage to the intestinal wall is currently considered as a promising therapeutic strategy to shorten postoperative dysmotility (1). Our work revisits the role of incoming monocytes in POI, showing that resolution of ME inflammation and postoperative recovery of GI motility depend upon a population of monocyte-derived MΦs with a pro-resolving phenotype that differentiate *in loco* from $CCR2^{+}$ inflammatory monocytes.

Leukocytes are recruited to the ME from the circulation a few hours after IM. This process is driven by chemokines secreted *in loco* and by adhesion molecules P-selectin, ICAM-1 and LFA-1 up-regulated on the endothelial surface within few hours after surgery (9;28). Until recently, infiltrating neutrophils and monocytes have been considered the main source of molecules that impair smooth muscle contraction, being responsible for the sustained inhibition of gastrointestinal motility (6;9;10). In line, pre-operative blocking of adhesion molecules such as ICAM-1 and LFA-1, reduced accumulation of leukocytes into the ME, normalized contractile response to the muscarinic agonist bethanecol *in vitro* and ameliorated gastric emptying *in vivo* 24 hours after surgery (6;9;10). However, the specific role played by the different immune cells in the pathogenesis of POI is not fully understood. Several studies reported that once recruited, leukocytes reside up to 7 days in the ME, even beyond the duration of POI, indeed suggesting that they may participate in resolution/recovery phase as well (9;29). Only recently, Stein et al have proposed a dual role for leukocytes recruited to the ME acting as pro-inflammatory cells over the first 24 hours after IM, able to cause tissue damage and functional impairment, but also playing a major role in the resolution process at a later stage (18).

Resolution of inflammation is a coordinated program in which monocyte-derived MΦs play an important role in containing immune-pathology, ceasing neutrophil recruitment, clearing damaged areas and inducing collagen deposition, revascularization, and recovery of tissue function via the secretion of anti-inflammatory cytokines and lipid mediators (14;15;30). In the context of POI, previous studies have already identified some anti-inflammatory mediators such as the immune-modulatory cytokine IL-10 and poly-unsaturated fatty acids (PUFA)-derived pro-resolving mediators involved in resolution of *muscularis* inflammation (18;31;32). Therefore, we hypothesized that, in line with other models of sterile inflammation, monocytes are essential for the resolution ME inflammation in POI.

Hence, in order to assess the role of incoming monocytes in POI, we employed intestinal manipulation in *Ccr2*$^{-/-}$ mice, lacking the CCR2 receptor and therefore unable to recruit CCR2-monocytes referred to as pro-inflammatory (20). Currently, murine intestinal manipulation of the intestine is widely used as a preclinical model of POI. This model recapitulates important clinical phenomena of the POI seen in surgical patients such as inflammatory response in the muscle layer of the intestine and delay of GI transit. Interestingly, functional and inflammatory parameters measured 24 hours after surgery in *Ccr2*$^{-/-}$ mice did not differ from those of control mice showing that preventing monocyte influx does not impact on the development of POI. Conversely, we observed a significant delay in the recovery of GI motility in *Ccr2*$^{-/-}$ mice, accompanied by more severe alterations of the neuromuscular function and increased inflammation. In fact, most of the *Ccr2*$^{-/-}$ mice only recovered 10 days after IM and in some cases these mice even succumb before complete recovery. In vitro, the effects of IM on muscle contractions were significantly potentiated, especially as EFS-induced contractions remained altered for several days after IM. Interestingly, prolonged neural dysfunction in *Ccr2*$^{-/-}$ mice was mirrored by typical signs of neuronal distress, as evidenced by the translocation of HuC/D to the nuclei of enteric neurons (22;23). Overall, neuromuscular alterations in *Ccr2*$^{-/-}$ mice were associated with an increased and long lasting expression of pro-inflammatory cytokines in the ME, resulting in augmented deposition of collagen

fibers and intra-abdominal adhesions. Considering the larger amount of IL-6^{+} and ROS^{+} neutrophils found in the ME of *Ccr2*$^{-/-}$ mice, it seemed likely that in the absence of monocyte-derived MΦs neutrophil clearance is impaired and the entire resolution process is disrupted, leading to a delayed functional recovery.

Furthermore, as for other models of sterile inflammation after acute injury, we demonstrated that also in POI inflammatory monocytes recruited to the ME acquired a pro-resolving phenotype. We showed indeed that IL-4 itself, and IL-4 target genes were expressed in the ME at very early time points after IM. In addition, anti-inflammatory genes *arg1*, *ym1* and *il10* and genes encoding for pro-resolving mediators such as *mrc1, stab1 and ym1* were found up-regulated at a later stage, mainly 3 days after IM. Cell sorting experiments confirmed the expression of these markers mainly in MHCII^{+} mature MΦs isolated from the ME 3 days after surgery. Of note, beside alternative activation of monocyte-derived MΦs, expansion of resident MΦs has been shown to be an important mechanism in sterile inflammatory models (33-37). Interestingly, we found that MΦs held proliferative activity and expanded *in situ*. Thus, we speculate that *muscularis* resident MΦs proliferate after surgical trauma. This would explain why MHCII^{lo} MΦs populated the injured ME of *Ccr2*$^{-/-}$ mice, albeit with significant delay compared to WT.

In conclusion, the results presented here suggest that monocyte recruitment is dispensable for the onset of POI. Hence, we favor the view that mainly ME resident MΦs activated during abdominal surgery release cytokines, prostaglandins and NO leading to impairment of neuromuscular function and ileus, and at the same time triggering the influx of inflammatory cells, mainly monocytes and neutrophils (38;39). Monocytes, entering the muscularis in a CCR2-dependent manner, will differentiate into MΦs resolving the inflammation and restoring intestinal function. Eventually, we showed that monocyte migration and differentiation to pro-resolving MΦs can be enhanced via CSF1 administration. Among the growth factors regulating monocyte/MΦ biology, CSF1 is an essential regulator of MΦ homeostasis (24), involved in monocyte entry into the

circulation (25;40) , monocyte/MΦ proliferation and polarization towards an immune-suppressive and tissue-repair phenotype (41). CSF1 treatment was in fact able to overcome the monocyte deficiency in *Ccr2*$^{-/-}$ mice, and thus promote repair and recovery after IM. In line, CSF1 has been shown to promote tissue recovery in models of ischemic damage to the kidneys (42), heart (43) and after partial hepatectomy (44) due to the presence of pro-resolving MΦ. In this context, CSF1-Fc fusion protein, with increased half-life and stability compared to recombinant CSF1, holds potential as a novel approach to accelerate recovery of POI (45).

Overall, from a therapeutic point of view, our findings imply that future therapies for POI should preferentially enhance tissue repair by promoting maturation of monocytes into MΦs with pro-resolving capacity rather than blocking recruitment of monocytes to the tissue.

Acknowledgments

The authors would like to thank I. Appeltans, J. Vandewalle and R. De Keyser (Translational Research Center for Gastrointestinal Disorders, KU Leuven, Belgium) for their excellent technical assistance.

Footnotes

Contributors

GF: acquisition of data, analysis and interpretation of data; drafting of the manuscript; PJG-P, MDG, EL, EM, FDE, MS, NS, YE, ZL, KS and DL: acquisition of data, analysis and interpretation of data; JVG and DAH: provided essential material and critical revision of the manuscript; GM and GEB: study concept and design; interpretation of data; obtained funding.

Grant support

This work was supported by grants from the Research Foundation – Flanders (FWO) (Odysseus program (G.0905.07) and FWO grant (G.0566.12N) to G.E.B, by a FWO PhD fellowship (to M.DG) and by FWO postdoctoral research fellowships (to G.M. and P.J.G).

Competing interests

The authors declare no financial, professional or personal conflicts relevant to the manuscript.

Ethics approval

Animal Care and Animal Experiments Committee of the University of Leuven (Leuven, Belgium)

Figure legends.

Figure 1. **Monocyte depletion does not prevent the development of POI.** WT and *Ccr2*$^{-/-}$ mice were subjected to IM and GI transit evaluated after 24 hours. (A) Dots represent geometric centre (GC) values of fluorescence distribution through the intestinal segments 90 minutes after oral administration of dextran-FITC in individual mice, mean ± SEM is also shown. WT and *Ccr2*$^{-/-}$ data sets of each condition were compared with their relative naïve control via unpaired t-test (*** $P <$ 0.0001). (B) Frequency and absolute numbers of $CD45^{+}CD11b^{+}Ly6G^{-}Ly6C^{hi}MHCII^{-}$ monocytes in WT (white bars) and *Ccr2*$^{-/-}$ mice (black bars) before and 1 day after IM. Data are shown as mean ± SEM. Statistical significance between WT and *Ccr2*$^{-/-}$ data sets was determined via unpaired t-test (*** $P <$ 0.0001 and ns= not significant). (C) Fold changes over naïve mic e of cytokine mRNA levels 1 day after IM are shown as mean ± SEM. Data sets were compared via unpaired t-test (* $P < 0.05$, ns= not significant). Data are representative of 3 independent experiments.

Figure 2. Preventing monocyte recruitment reduces smooth muscle contraction, GI motility *in vivo* and affects survival after intestinal manipulation. WT and *Ccr2*$^{-/-}$ mice were subjected to IM and GI transit was assessed 1, 3, 5 and 10 days after IM. (A) Graph represents GC values mean ± SEM from WT and *Ccr2*$^{-/-}$ mice at indicated time point after IM. WT and *Ccr2*$^{-/-}$ data sets were compared with two-way ANOVA test followed by Bonferroni correction (** $P < 0.001$, *** $P < 0.0001$ and ns= not significant). Data are representative of 3 independent experiments. (B) Percentage survival rate shown as a Kaplan-Meier survival curve. Survival curves were compared via Gehan-Breslow-Wilcoxon test (* $P < 0.05$). (C-E) Ileal smooth muscle strips from WT and *Ccr2*$^{-/-}$ mice at 1, 3 and 5 days after IM were stimulated *in vitro* to assess myogenic and neurogenic contractions. Each data set includes 6 mice. Data are representative of 3 independent experiments. (C) Mean values (in mN/mm^2) ± SEM of contractile responses to KCl (60 mM). WT and *Ccr2*$^{-/-}$ data sets were compared at each time point via unpaired t-test (** $P < 0.001$ and ns= not significant). (D) Mean values (in mN/mm^2) ± SEM of contractile responses to increasing concentrations of carbachol (CCh). WT and

Ccr2$^{-/-}$ dose response curves were compared via two-way ANOVA test followed by Bonferroni correction (** P < 0.001, ns= not significant). (E) Mean values (in mN/mm^2) ± SEM of contractile responses to EFS at increasing frequencies. WT and *Ccr2*$^{-/-}$ frequency- response curves were compared via two-way ANOVA test followed by Bonferroni correction (* P < 0.05 and ** P < 0.001).

Figure 3. Lack of CCR2-monocytes induces enteric neuronal alteration after intestinal manipulation. WT and *Ccr2*$^{-/-}$ mice were subjected to IM and the myenteric plexus and enteric neurons analysed 5 days after IM. (A) Representative confocal images of whole mount ME preparations from WT and *Ccr2*$^{-/-}$ mice. Neuronal cell bodies are identified via HuC/D (red), the interganglionic connections via neurofilament (NF200; green) and nuclei using DAPI (blue), scale bar is 20µm. (B) Volume of individual HuC/D$^+$ enteric neurons in WT and *Ccr2*$^{-/-}$ mice 5 days after IM are represented, mean are shown for both groups as white line. (C) Fluorescent intensity of HuC/D in individual enteric neuronal nuclei is shown. (D) Percentage of HuC/D fluorescent intensity in the nucleus of individual enteric neuronal nuclei versus the total cellular HuC/D is shown, median are shown for both groups as white line. WT and *Ccr2*$^{-/-}$ data sets were compared via unpaired t-test (*** *P* < 0.001, ns= not significant).

Figure 4. Persistent inflammation, neutrophil-mediated pathology and increased fibrosis in *Ccr2*$^{-/-}$ mice after IM. WT and *Ccr2*$^{-/-}$ mice were subjected to IM and inflammatory parameters were analyzed at day 3. (A) Fold changes over naïve mice of cytokine mRNA levels 3 days after IM are shown as mean ± SEM. Data sets were compared via unpaired t-test (* *P* < 0.05, ** *P* < 0.001, ns= not significant). (B) Absolute numbers of CD11b$^+$Ly6G$^+$ neutrophils, ROS$^+$ neutrophils, IL-6$^+$ neutrophils and TNFα$^+$ neutrophils isolated 1 and 3 days after IM. WT and *Ccr2*$^{-/-}$ were compared at both time points via unpaired t-test (*** *P* < 0.0001), data are representative of 3 independent experiments. (C) Representative images of Masson's trichrome staining in small intestine cross sections of naïve WT and *Ccr2*$^{-/-}$ mice and at 5 days after IM. (D) Measurements of *muscularis* thickness are shown as mean ± SEM for naïve mice and 5 days after IM. Data sets were compared

with naïve via unpaired t-test (* $P < 0.05$). WT and *Ccr2*$^{-/-}$ data sets were compared at both time points via unpaired t-test (* $P < 0.05$ and ns= not significant). (E) Percentages of collagen in small intestine cross sections are shown as mean values ± SEM. WT and *Ccr2*$^{-/-}$ mice were compared at both time points via unpaired t-test (* $P < 0.05$, ns= not significant). (F) Peritoneal adhesions were scored in WT and *Ccr2*$^{-/-}$ mice before and 5 days after IM. WT and *Ccr2*$^{-/-}$ data sets were compared at both time points via unpaired t-test (* $P < 0.05$, ns= not significant).

Figure 5. Mature macrophages accumulate into the *muscularis externa* during recovery. Immune cells isolated from the ME of naïve WT and *Ccr2*$^{-/-}$ mice and 1, 3 and 5 days after IM were analyzed via flow cytometry. (A) Representative dot plot showing CD11b^{+}Ly6G^{+} neutrophils and CD11b^{+}Ly6G^{-} cells gated on the CD45^{+} population. Ly6C^{hi}MHCII^{-} monocytes, Ly6C^{+}MHCII^{+} immature MΦs, and Ly6C^{-}MHCII^{lo} and Ly6C^{-}MHCII^{hi} MΦs were gated on the CD11b^{+}Ly6G^{-} population. Absolute numbers of neutrophils (B), Ly6C^{hi}MHCII^{-} monocytes (C), Ly6C^{+}MHCII^{+} immature MΦs (D) and Ly6C^{-}MHCII^{lo} (E), and Ly6C^{-}MHCII^{hi} MΦs (F), in WT (white bars) and *Ccr2*$^{-/-}$ mice (black bars). Data are shown as mean ± SEM. Statistical significance between WT and *Ccr2*$^{-/-}$ data sets was determined via unpaired t-test (* $P < 0.05$, ** $P < 0.001$, *** $P < 0.0001$ and ns= not significant) data are representative of 3 independent experiments.

Figure 6. Mature macrophages originate from CCR2^{+} monocytes and from proliferating resident macrophages. Ly6C^{hi} monocytes were isolated from UBI-GFP reporter mice and injected i.v. into WT mice 1 hr before IM to trace monocyte differentiation *in situ*. (A) Dot plot representing GFP^{+} cells in the ME of naïve mice and at 1, 3 and 5 days after IM. (B) Frequencies of Ly6C^{hi}MHCII^{-} monocytes, Ly6C^{+}MHCII^{+} immature MΦs, Ly6C^{-}MHCII^{lo} and Ly6C^{-}MHCII^{hi} MΦs within the GFP^{+} cells. Data are shown as mean ± SEM. Data are representative of 2 independent experiments. (C) A pulse of BrdU was given to naïve WT mice and at 1, 3 and 5 days after IM. Proliferation rate of immune cells isolated from ME was assessed via FACS analysis. (C) Absolute numbers of BrdU positive Ly6C^{hi}MHCII^{-} monocytes, Ly6C^{+}MHCII^{+} immature MΦs and Ly6C^{-}MHCII^{lo} or Ly6C^{-}MHCII^{hi} MΦs. (D) Ki67 staining

was assessed in naïve WT mice and at 1, 3 and 5 days after IM. Proliferation rate of immune cells isolated from ME was assessed via FACS analysis. (D) Absolute numbers of Ki67 positive Ly6C^{hi}MHCII^{-} monocytes, Ly6C^{+}MHCII^{+} immature MΦs and Ly6C^{-}MHCII^{lo} or Ly6C^{-}MHCII^{hi} MΦs. Each data set included 6 mice. Data are shown as mean ± SEM representative of 2 independent experiments. All data sets were compared to data in naïve mice via one-way ANOVA followed by Dunnett's Multiple Comparison Test (* $P < 0.05$, ** $P < 0.001$ and *** $P < 0.0001$).

Figure 7. Monocyte-derived macrophages hold a pro-resolving phenotype. Gene expression levels of pro-inflammatory and pro-resolving markers were measured in homogenates of ME of WT mice at different time points after IM (A), and in monocytes and MΦs isolated via cell sorting from the ME of WT mice 3 days after IM (B). In A data are expressed as fold change mean values ± SEM over naïve mice. In B mRNA levels (mean values ± SEM) in sorted monocytes and MΦs expressed as relative expression of the gene of interest over the expression of the reference gene *rpl32*. Data are representative of 3 independent experiments.

Figure 8. CSF1 drives pro-resolving macrophage differentiation and favours recovery of GI motility. WT and Ccr2$^{-/-}$ mice undergoing IM were treated with either (0.75 µg/g) CSF1-Fc or saline. Functional and inflammatory parameters were assessed 3 days after IM. (A) Absolute numbers of Ly6C^{hi}MHCII^{-} monocytes, Ly6C^{+}MHCII^{+} immature MΦs, Ly6C^{-}MHCII^{lo} and Ly6C^{-}MHCII^{hi} MΦs in WT and *Ccr2*$^{-/-}$ mice. Statistical significance between CSF1-Fc and saline-treated data sets was determined via unpaired t-test (* $P < 0.05$, ** $P < 0.001$, *** $P < 0.0001$ and ns= not significant). (B) Absolute numbers of ROS^{+} neutrophils. Statistical significance between CSF1-Fc and saline-treated data sets was determined via unpaired t-test (** $P < 0.001$). (C) Dots represent GC values from individual mice; mean ± SEM are also shown. Statistical significance between CSF1-Fc and saline-treated data sets was determined via unpaired t-test (* $P < 0.05$).

Reference List

(1) Boeckxstaens GE, de Jonge WJ. Neuroimmune mechanisms in postoperative ileus. *Gut* 2009;**58**(9):1300-11.

(2) Asgeirsson T, El-Badawi KI, Mahmood A *et al*. Postoperative ileus: it costs more than you expect. *Journal of the American College of Surgeons* 2010;**210**(2):228-31.

(3) Mikkelsen HB, Thuneberg L, Rumessen JJ *et al*. Macrophage-like cells in the muscularis externa of mouse small intestine. *Anat Rec* 1985;**213**(1):77-86.

(4) Kalff JC, Turler A, Schwarz NT *et al*. Intra-abdominal activation of a local inflammatory response within the human muscularis externa during laparotomy. *Ann Surg* 2003;**237**(3):301-15.

(5) Muller PA, Koscso B, Rajani GM *et al*. Crosstalk between muscularis macrophages and enteric neurons regulates gastrointestinal motility. *Cell* 2014;**158**(2):300-13.

(6) de Jonge WJ, van den Wijngaard RM, The FO *et al*. Postoperative ileus is maintained by intestinal immune infiltrates that activate inhibitory neural pathways in mice. *Gastroenterology* 2003;**125**(4):1137-47.

(7) Wehner S, Behrendt FF, Lyutenski BN *et al*. Inhibition of macrophage function prevents intestinal inflammation and postoperative ileus in rodents. *Gut* 2007;**56**(2):176-85.

(8) Matteoli G, Gomez-Pinilla PJ, Nemethova A *et al*. A distinct vagal anti-inflammatory pathway modulates intestinal muscularis resident macrophages independent of the spleen. *Gut* 2014;**63**(6):938-48.

(9) Kalff JC, Carlos TM, Schraut WH *et al*. Surgically induced leukocytic infiltrates within the rat intestinal muscularis mediate postoperative ileus. *Gastroenterology* 1999;**117**(2):378-87.

(10) The FO, de Jonge WJ, Bennink RJ *et al*. The ICAM-1 antisense oligonucleotide ISIS-3082 prevents the development of postoperative ileus in mice. *Br J Pharmacol* 2005;**146**(2):252-8.

(11) Shechter R, London A, Varol C *et al*. Infiltrating blood-derived macrophages are vital cells playing an anti-inflammatory role in recovery from spinal cord injury in mice. *PLoS Med* 2009;**6**(7):e1000113.

(12) Zigmond E, Samia-Grinberg S, Pasmanik-Chor M *et al*. Infiltrating monocyte-derived macrophages and resident kupffer cells display different ontogeny and functions in acute liver injury. *J Immunol* 2014;**193**(1):344-53.

(13) Nahrendorf M, Pittet MJ, Swirski FK. Monocytes: protagonists of infarct inflammation and repair after myocardial infarction. *Circulation* 2010;**121**(22):2437-45.

(14) Grainger JR, Wohlfert EA, Fuss IJ *et al*. Inflammatory monocytes regulate pathologic responses to commensals during acute gastrointestinal infection. *Nat Med* 2013;**19**(6):713-21.

(15) Serhan CN, Savill J. Resolution of inflammation: the beginning programs the end. *Nat Immunol* 2005;**6**(12):1191-7.

(16) Stoffels B, Schmidt J, Nakao A *et al*. Role of interleukin 10 in murine postoperative ileus. *Gut* 2009;**58**(5):648-60.

(17) Wehner S, Meder K, Vilz TO *et al*. Preoperative short-term parenteral administration of polyunsaturated fatty acids ameliorates intestinal inflammation and postoperative ileus in rodents. *Langenbecks Arch Surg* 2012;**397**(2):307-15.

(18) Stein K, Stoffels M, Lysson M *et al*. A role for 12/15-lipoxygenase-derived proresolving mediators in postoperative ileus: protectin DX-regulated neutrophil extravasation. *J Leukoc Biol* 2016;**99**(2):231-9.

(19) van Bree SH, Nemethova A, van Bovenkamp FS *et al*. Novel method for studying postoperative ileus in mice. *Int J Physiol Pathophysiol Pharmacol* 2012;**4**(4):219-27.

(20) Kurihara T, Warr G, Loy J *et al*. Defects in macrophage recruitment and host defense in mice lacking the CCR2 chemokine receptor. *J Exp Med* 1997;**186**(10):1757-62.

(21) Farro G, Gomez-Pinilla PJ, Di GM *et al*. Smooth muscle and neural dysfunction contribute to different phases of murine postoperative ileus. *Neurogastroenterol Motil* 2016;**28**(6):934-47.

(22) Cirillo C, Bessissow T, Desmet AS *et al*. Evidence for neuronal and structural changes in submucous ganglia of patients with functional dyspepsia. *Am J Gastroenterol* 2015;**110**(8):1205-15.

(23) Desmet AS, Cirillo C, Vanden Berghe P. Distinct subcellular localization of the neuronal marker HuC/D reveals hypoxia-induced damage in enteric neurons. *Neurogastroenterol Motil* 2014;**26**(8):1131-43.

(24) Stanley ER, Cifone M, Heard PM *et al*. Factors regulating macrophage production and growth: identity of colony-stimulating factor and macrophage growth factor. *J Exp Med* 1976;**143**(3):631-47.

(25) Hume DA, Pavli P, Donahue RE *et al*. The effect of human recombinant macrophage colony-stimulating factor (CSF-1) on the murine mononuclear phagocyte system in vivo. *J Immunol* 1988;**141**(10):3405-9.

(26) Gow DJ, Sauter KA, Pridans C *et al*. Characterisation of a novel Fc conjugate of macrophage colony-stimulating factor. *Mol Ther* 2014;**22**(9):1580-92.

(27) Bauer AJ, Boeckxstaens GE. Mechanisms of postoperative ileus. *Neurogastroenterol Motil* 2004;**16 Suppl 2**:54-60.

(28) Kalff JC, Schraut WH, Simmons RL *et al*. Surgical manipulation of the gut elicits an intestinal muscularis inflammatory response resulting in postsurgical ileus. *Ann Surg* 1998;**228**(5):652-63.

(29) Wehner S, Vilz TO, Stoffels B *et al*. Immune mediators of postoperative ileus. *Langenbecks Arch Surg* 2012;**397**(4):591-601.

(30) Serhan CN, Chiang N, Dalli J *et al*. Lipid mediators in the resolution of inflammation. *Cold Spring Harb Perspect Biol* 2015;**7**(2):a016311.

(31) Stoffels B, Schmidt J, Nakao A *et al*. Role of interleukin 10 in murine postoperative ileus. *Gut* 2009;**58**(5):648-60.

(32) Wehner S, Meder K, Vilz TO *et al*. Preoperative short-term parenteral administration of polyunsaturated fatty acids ameliorates intestinal inflammation and postoperative ileus in rodents. *Langenbecks Arch Surg* 2012;**397**(2):307-15.

(33) Little MC, Hurst RJ, Else KJ. Dynamic changes in macrophage activation and proliferation during the development and resolution of intestinal inflammation. *J Immunol* 2014;**193**(9):4684-95.

(34) Van GN, Van OE, Leuckx G *et al*. Macrophage dynamics are regulated by local macrophage proliferation and monocyte recruitment in injured pancreas. *Eur J Immunol* 2015;**45**(5):1482-93.

(35) Davies LC, Rosas M, Jenkins SJ *et al*. Distinct bone marrow-derived and tissue-resident macrophage lineages proliferate at key stages during inflammation. *Nat Commun* 2013;**4**:1886.

(36) Jenkins SJ, Ruckerl D, Thomas GD *et al*. IL-4 directly signals tissue-resident macrophages to proliferate beyond homeostatic levels controlled by CSF-1. *J Exp Med* 2013;**210**(11):2477-91.

(37) Jenkins SJ, Ruckerl D, Cook PC *et al*. Local macrophage proliferation, rather than recruitment from the blood, is a signature of TH2 inflammation. *Science* 2011;**332**(6035):1284-8.

(38) Kalff JC, Schraut WH, Billiar TR *et al*. Role of inducible nitric oxide synthase in postoperative intestinal smooth muscle dysfunction in rodents. *Gastroenterology* 2000;**118**(2):316-27.

(39) Hori M, Kita M, Torihashi S *et al*. Upregulation of iNOS by COX-2 in muscularis resident macrophage of rat intestine stimulated with LPS. *Am J Physiol Gastrointest Liver Physiol* 2001;**280**(5):G930-G938.

(40) Van OE, Stijlemans B, Heymann F *et al*. M-CSF and GM-CSF Receptor Signaling Differentially Regulate Monocyte Maturation and Macrophage Polarization in the Tumor Microenvironment. *Cancer Res* 2016;**76**(1):35-42.

(41) Martinez FO, Gordon S, Locati M *et al*. Transcriptional profiling of the human monocyte-to-macrophage differentiation and polarization: new molecules and patterns of gene expression. *J Immunol* 2006;**177**(10):7303-11.

(42) Alikhan MA, Jones CV, Williams TM *et al*. Colony-stimulating factor-1 promotes kidney growth and repair via alteration of macrophage responses. *Am J Pathol* 2011;**179**(3):1243-56.

(43) Okazaki T, Ebihara S, Asada M *et al*. Macrophage colony-stimulating factor improves cardiac function after ischemic injury by inducing vascular endothelial growth factor production and survival of cardiomyocytes. *Am J Pathol* 2007;**171**(4):1093-103.

(44) Stutchfield BM, Antoine DJ, Mackinnon AC *et al*. CSF1 Restores Innate Immunity After Liver Injury in Mice and Serum Levels Indicate Outcomes of Patients With Acute Liver Failure. *Gastroenterology* 2015;**149**(7):1896-909.

(45) Hume DA, MacDonald KP. Therapeutic applications of macrophage colony-stimulating factor-1 (CSF-1) and antagonists of CSF-1 receptor (CSF-1R) signaling. *Blood* 2012;**119**(8):1810-20.

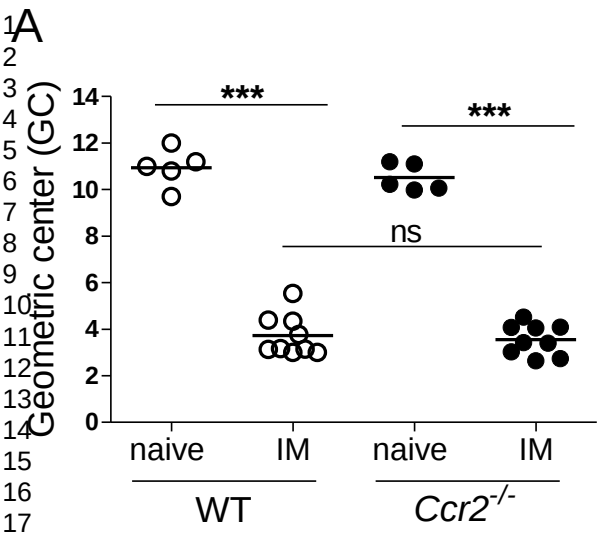
A
Geometric center (GC)
***
***
ns
naive
IM
naive
IM
WT
Ccr2-/-

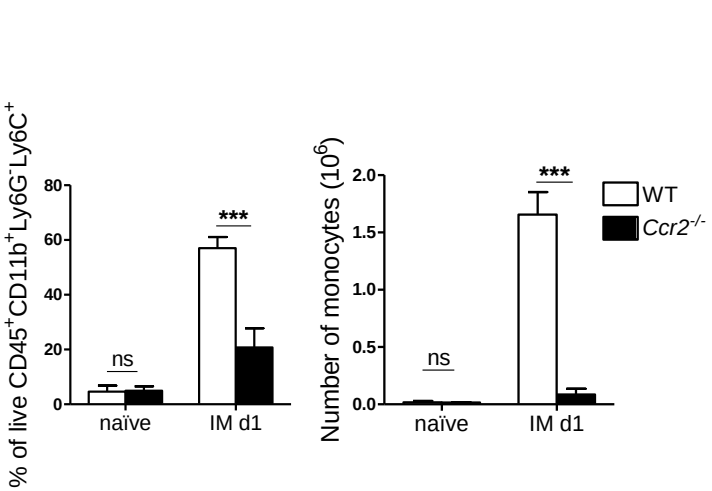
B
% of live CD45+CD11b+Ly6G-Ly6C+
***
ns
naïve
IM d1
Number of monocytes (10^6)
***
ns
naïve
IM d1
WT
Ccr2-/-

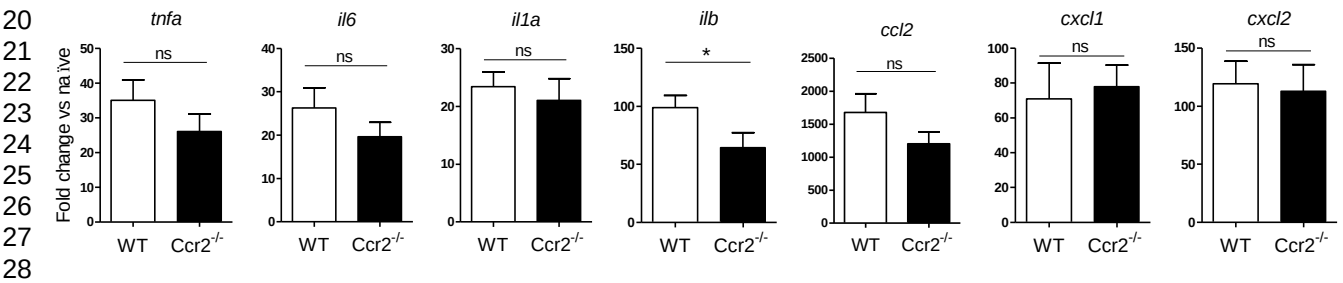
C
tnfa
il6
il1a
ilb
ccl2
cxcl1
cxcl2
Fold change vs naive
ns
*
WT
Ccr2-/-

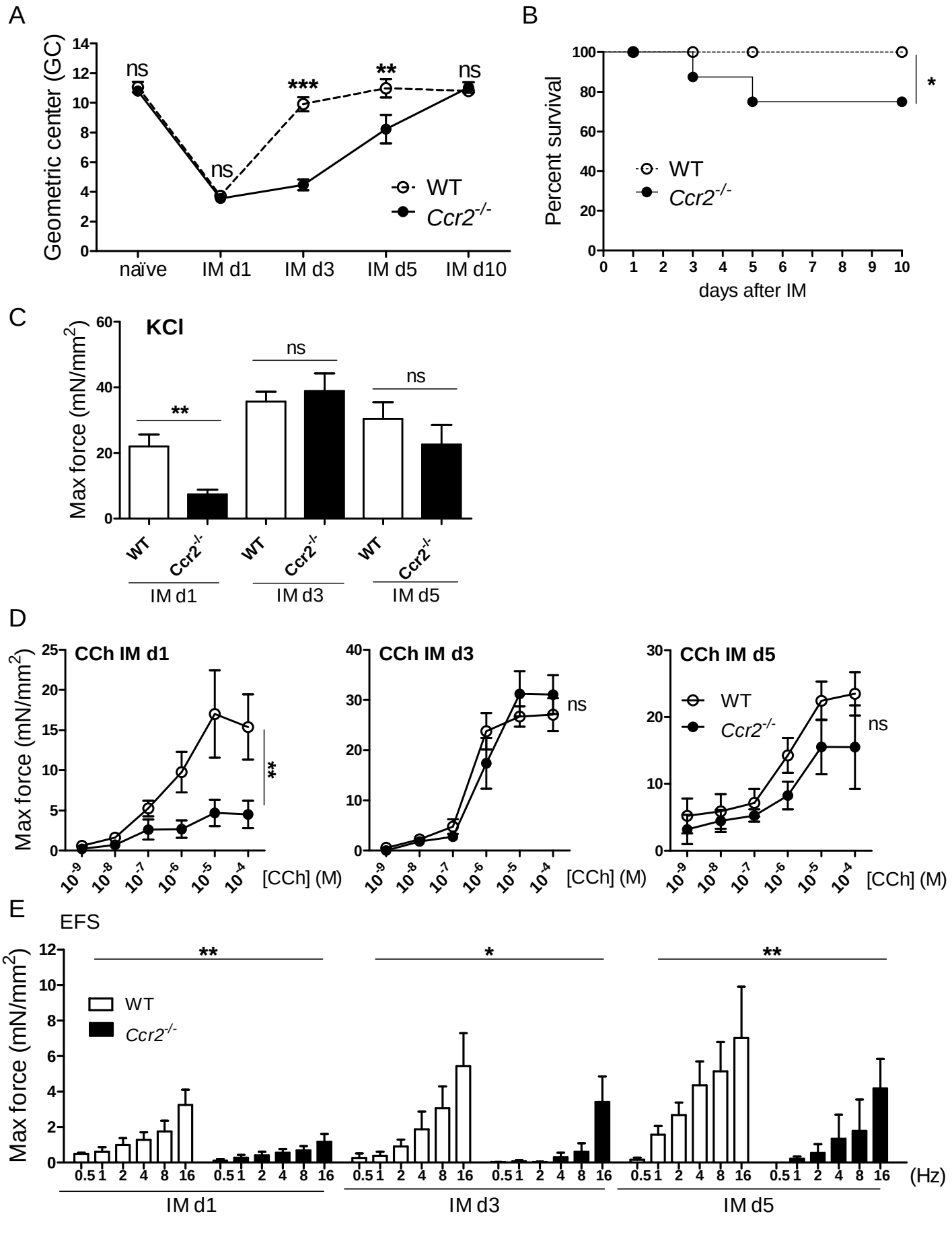
A
Geometric center (GC)
ns
***
**
ns
ns
WT
Ccr2-/-
naïve
IM d1
IM d3
IM d5
IM d10
B
Percent survival
WT
Ccr2-/-
*
days after IM
C
KCl
Max force (mN/mm2)
**
ns
ns
WT
Ccr2-/-
IM d1
IM d3
IM d5
D
CCh IM d1
CCh IM d3
CCh IM d5
Max force (mN/mm2)
**
ns
ns
WT
Ccr2-/-
[CCh] (M)
E
EFS
Max force (mN/mm2)
**
*
**
WT
Ccr2-/-
0.5 1 2 4 8 16
(Hz)
IM d1
IM d3
IM d5

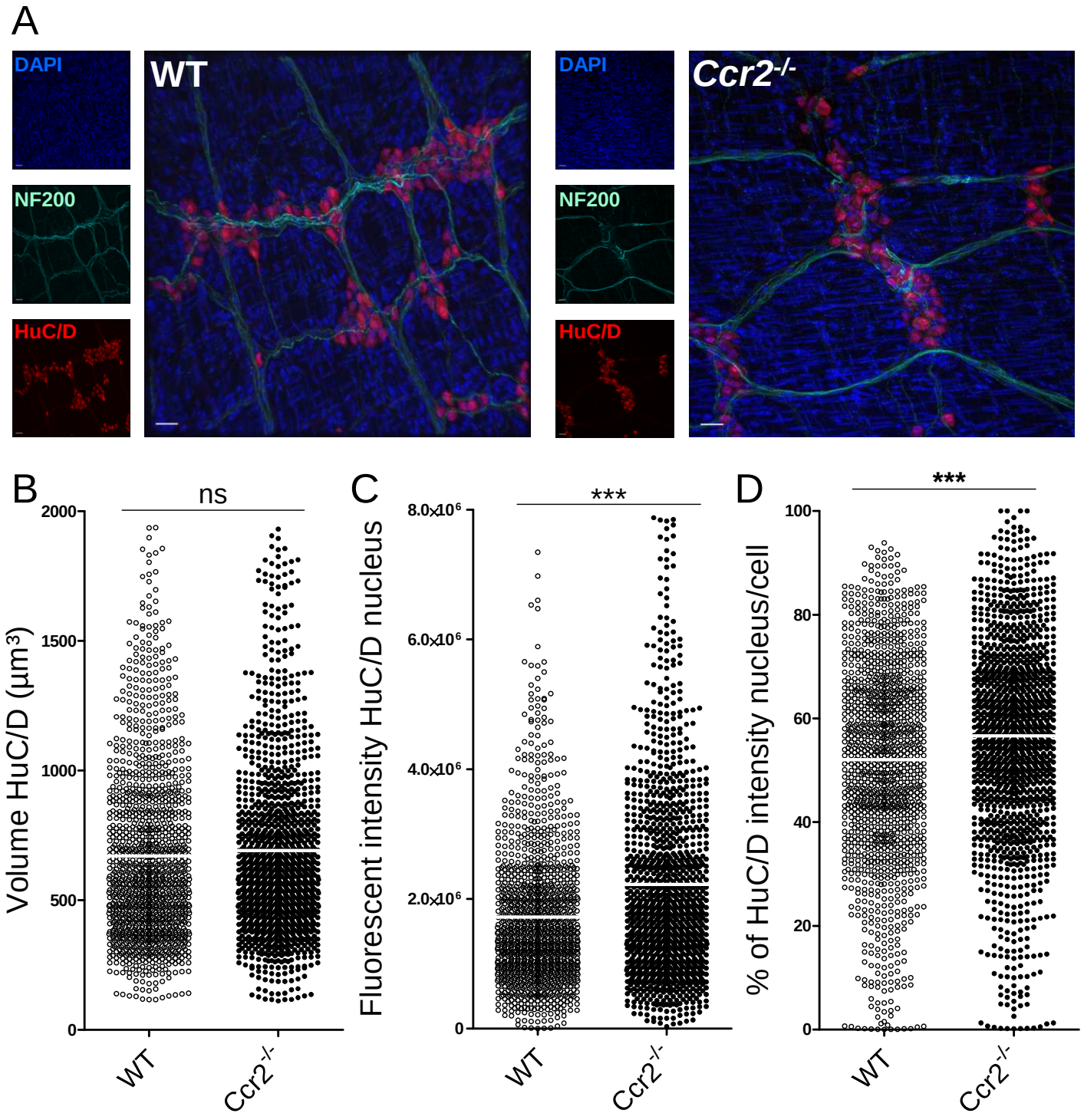
A
DAPI
NF200
HuC/D
WT
DAPI
NF200
HuC/D
Ccr2-/-
B
ns
Volume HuC/D (µm³)
2000
1500
1000
500
0
WT
Ccr2-/-
C
***
Fluorescent intensity HuC/D nucleus
8.0x10⁶
6.0x10⁶
4.0x10⁶
2.0x10⁶
0
WT
Ccr2-/-
D
***
% of HuC/D intensity nucleus/cell
100
80
60
40
20
0
WT
Ccr2-/-

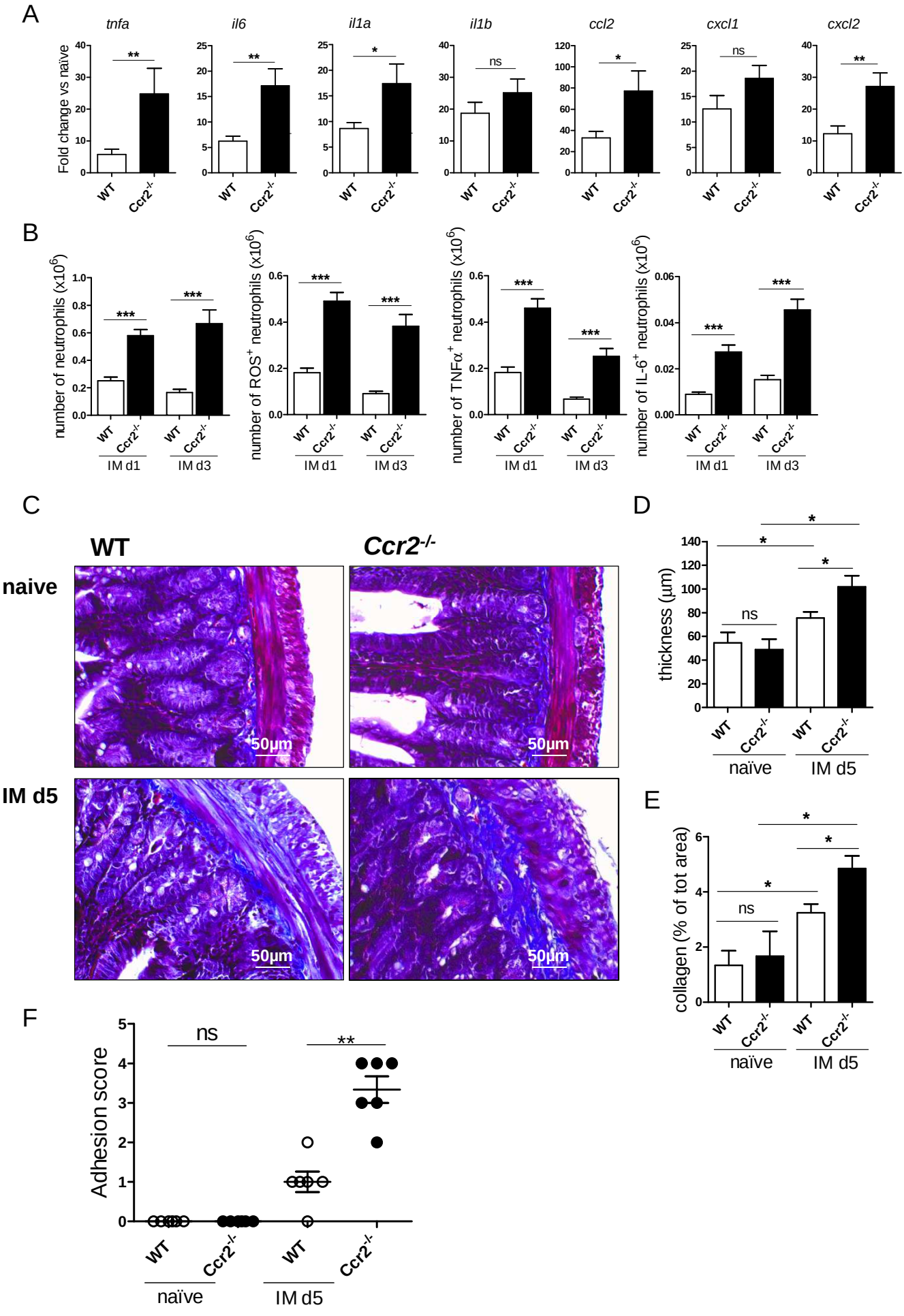
A
tnfa
il6
il1a
il1b
ccl2
cxcl1
cxcl2
Fold change vs naïve
WT
Ccr2-/-
B
number of neutrophils (x10^6)
number of ROS+ neutrophils (x10^6)
number of TNFα+ neutrophils (x10^6)
number of IL-6+ neutrophils (x10^6)
IM d1
IM d3
C
WT
Ccr2-/-
naive
IM d5
50µm
D
thickness (µm)
naïve
IM d5
E
collagen (% of tot area)
F
Adhesion score

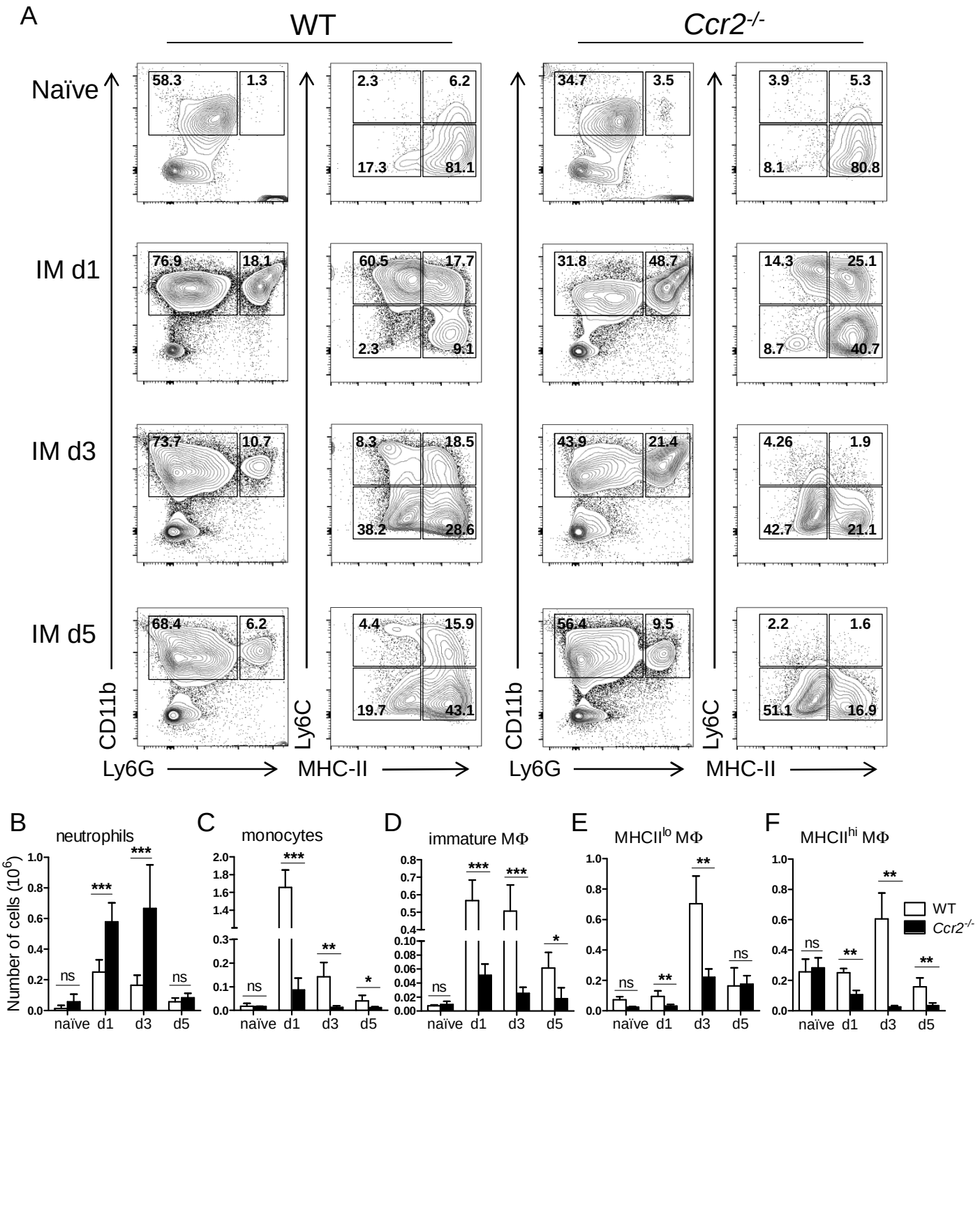
A
WT
Ccr2-/-
Naïve
IM d1
IM d3
IM d5
58.3
1.3
2.3
6.2
17.3
81.1
34.7
3.5
3.9
5.3
8.1
80.8
76.9
18.1
60.5
17.7
2.3
9.1
31.8
48.7
14.3
25.1
8.7
40.7
73.7
10.7
8.3
18.5
38.2
28.6
43.9
21.4
4.26
1.9
42.7
21.1
68.4
6.2
4.4
15.9
19.7
43.1
56.4
9.5
2.2
1.6
51.1
16.9
CD11b
Ly6G
Ly6C
MHC-II
B
neutrophils
C
monocytes
D
immature MΦ
E
MHCIIlo MΦ
F
MHCIIhi MΦ
Number of cells (10^6)
WT
Ccr2-/-
ns
naïve
d1
d3
d5

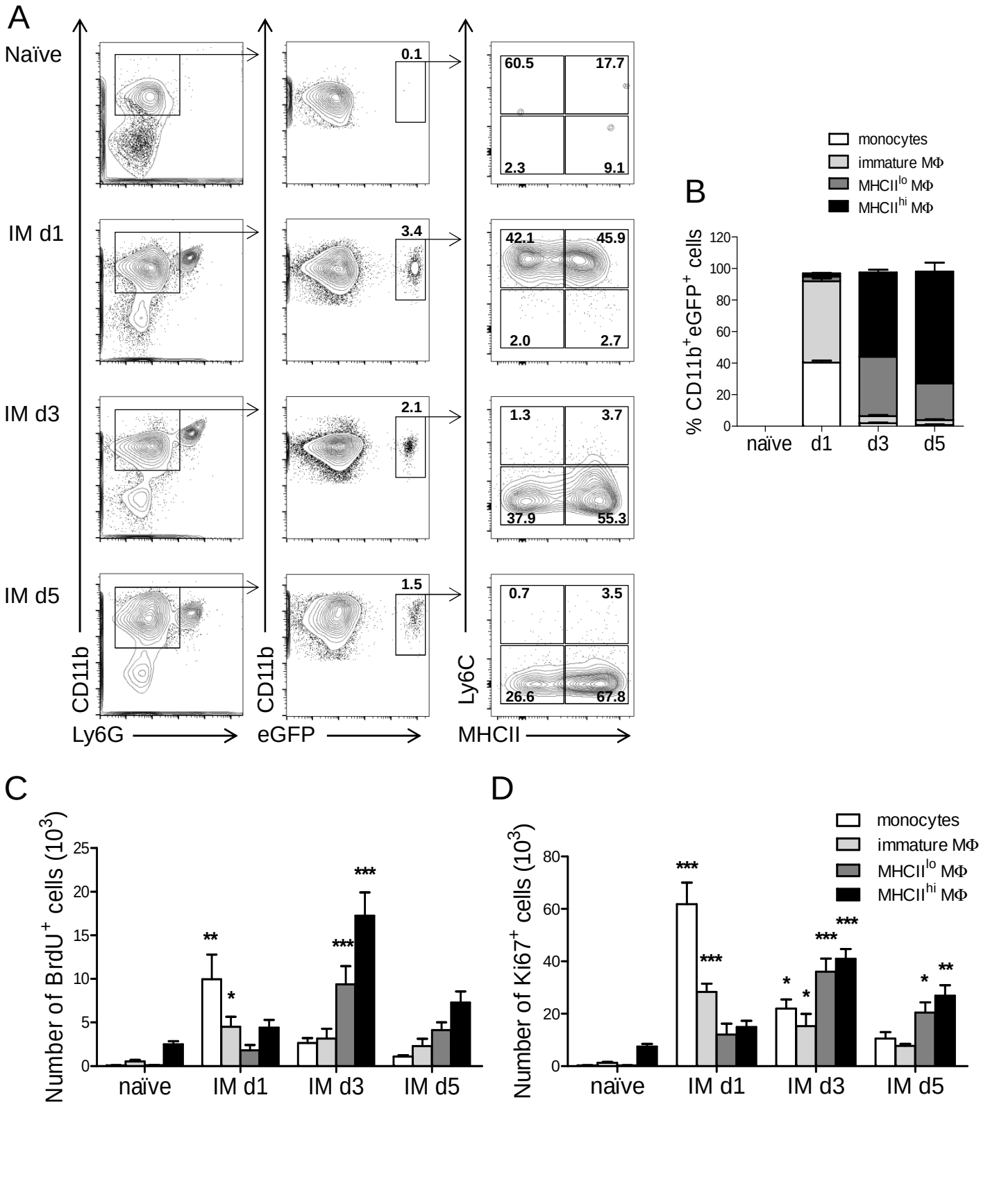
A
Naïve
IM d1
IM d3
IM d5
0.1
60.5
17.7
2.3
9.1
3.4
42.1
45.9
2.0
2.7
2.1
1.3
3.7
37.9
55.3
1.5
0.7
3.5
26.6
67.8
CD11b
Ly6G
CD11b
eGFP
Ly6C
MHCII
B
monocytes
immature MΦ
MHCII^lo MΦ
MHCII^hi MΦ
% CD11b+eGFP+ cells
120
100
80
60
40
20
0
naïve
d1
d3
d5
C
Number of BrdU+ cells (10^3)
25
20
15
10
5
0
**
*
***
***
naïve
IM d1
IM d3
IM d5
D
Number of Ki67+ cells (10^3)
80
60
40
20
0
***
***
*
*
***
***
*
**
monocytes
immature MΦ
MHCII^lo MΦ
MHCII^hi MΦ
naïve
IM d1
IM d3
IM d5

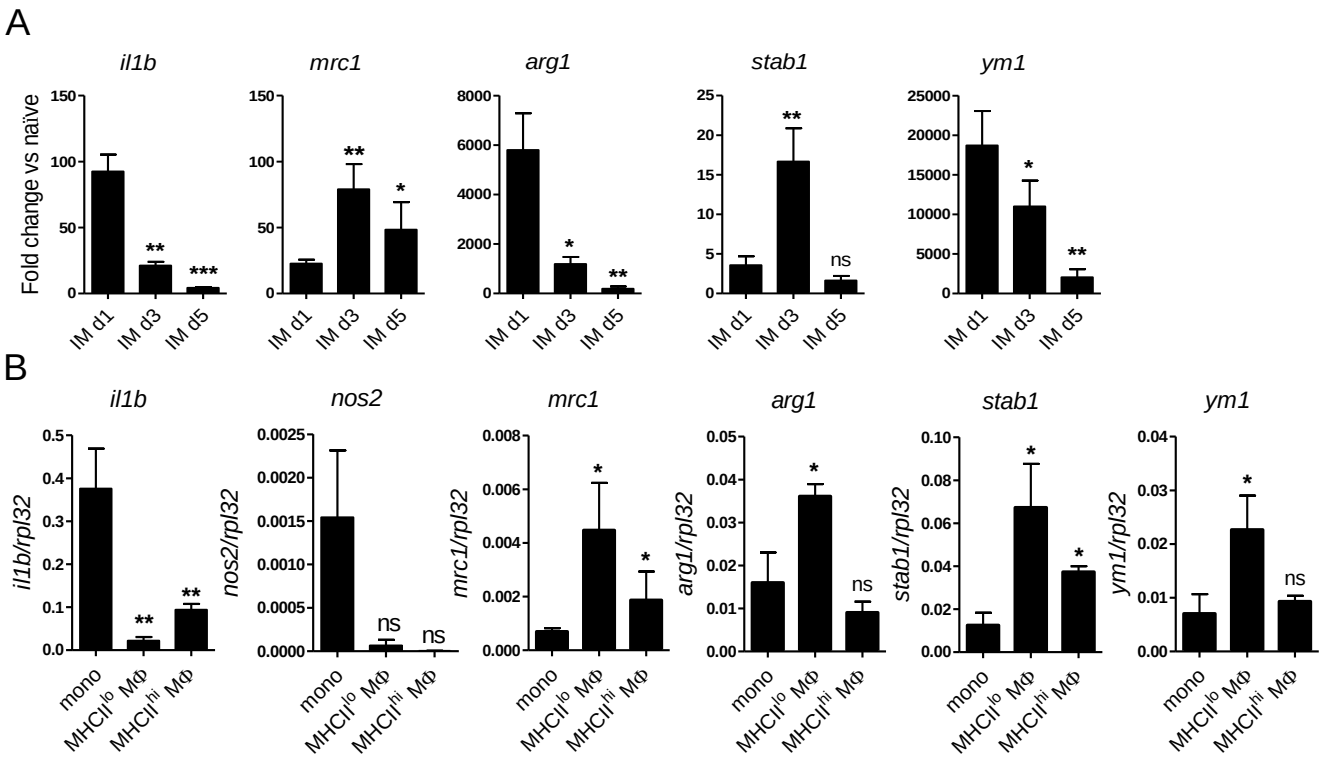
A
il1b
mrc1
arg1
stab1
ym1
Fold change vs naïve
IM d1
IM d3
IM d5
B
il1b/rpl32
nos2/rpl32
mrc1/rpl32
arg1/rpl32
stab1/rpl32
ym1/rpl32
nos2
mono
MHCII^lo Mϕ
MHCII^hi Mϕ
ns

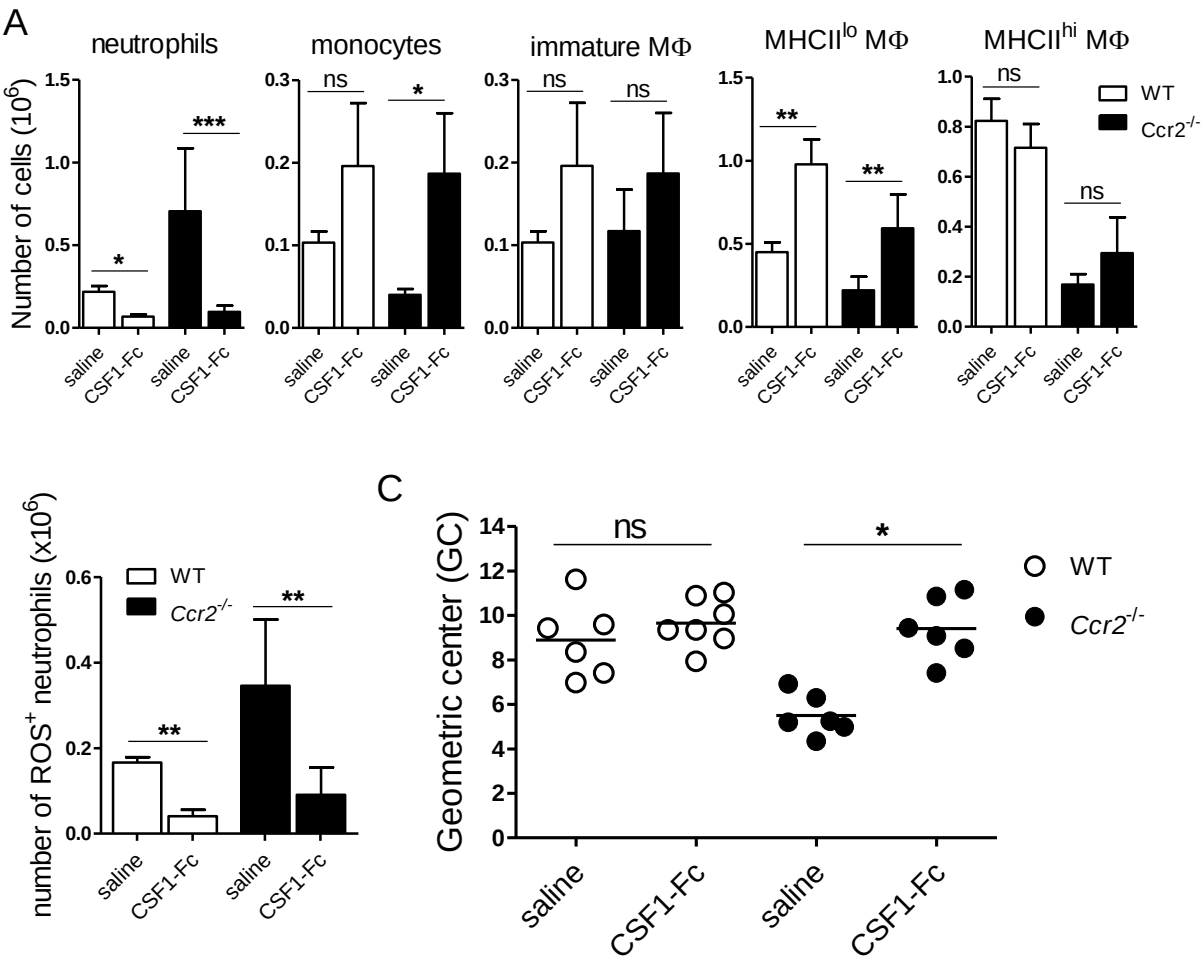
A
neutrophils
monocytes
immature MΦ
MHCII^lo MΦ
MHCII^hi MΦ
Number of cells (10^6)
WT
Ccr2^-/-
ns
*
**
***
saline
CSF1-Fc

B
number of ROS^+ neutrophils (x10^6)
WT
Ccr2^-/-
**
saline
CSF1-Fc

C
Geometric center (GC)
ns
*
WT
Ccr2^-/-
saline
CSF1-Fc

Farro et al.

Supplementary material and figures to:

CCR2-dependent monocyte-derived macrophages resolve inflammation and restore gut motility in postoperative ileus.

Short title: Macrophages resolve postoperative ileus

Giovanna Farro[1], Michelle Stakenborg[1], Pedro J Gomez-Pinilla[1], Evelien Labeeuw[1], Gera Goverse[1], Martina Di Giovangiulio[1], Nathalie Stakenborg[1], Elisa Meroni[1], Francesca D'Errico[1], Yvon Elkrim[2,3], Damya Laoui[2,3], Zofia M. Lisowski[4], Kristin A. Sauter[4], David A. Hume[4], Jo A. Van Ginderachter[2,3], Guy E. Boeckxstaens[1#] & Gianluca Matteoli[1#].

[1]KU Leuven Department of Clinical and Experimental Medicine, Translational Research Center for Gastrointestinal Disorders (TARGID), Leuven, Belgium. [2] Myeloid Cell Immunology Lab, VIB Inflammation Research Center, Ghent, Belgium. [3] Lab of Cellular and Molecular Immunology, Vrije Universiteit Brussel, Pleinlaan 2, B-1050 Brussels, Belgium. [4]The Roslin Institute and Royal (Dick) School of Veterinary Studies, University of Edinburgh, Easter Bush, EH25 9RG, UK.

[#] These authors contributed equally as co-last authors.

Corresponding authors:

Prof. Gianluca Matteoli & **Prof. Guy E. Boeckxstaens**
Department of Clinical and Experimental Medicine
Translational Research Center for Gastrointestinal Disorders (TARGID)
KU Leuven; Herestraat 49, O&N1, bus 701; 3000, Leuven, Belgium
Tel: +32-16-330238/ +32-16-345750

E-mail: **gianluca.matteoli@kuleuven.be** and **guy.boeckxstaens@kuleuven.be**

Supplementary material and methods

Gastrointestinal transit measurement

To assess GI transit, 10 µl of a liquid non-absorbable fluorescein isothiocyanate-labeled dextran (FITC-dextran, 70,000 Da; Invitrogen) was administered by oral gavage to fasted animals. Ninety minutes later, animals were sacrificed by CO_2 overdose and the content of stomach, small bowel (divided in 10 segments of equal length), caecum, and colon (divided in 3 segments of equal length) was collected for quantification of fluorescence using a spectrofluorimeter (Ascent, Labsystem Inc) at 488 nm. The distribution of the fluorescent dextran along the GI tract was determined by calculating the geometric center (GC): Σ (percent of total fluorescent signal in each segment x the segment number)/100 for quantitative comparison among experimental groups (1).

Adhesion formation

Formation of adhesions in the peritoneal cavity after intestinal manipulation was quantified by assessing adhesions at day 5 after surgery. A previously described adhesion score was used: score 0, no adhesions; score 1, thin, pellucid adhesions; score 2, tensile adhesion; score 3, inseparable and vascularized adhesion; score 4, entire abdomen linked by adhesions (2).

Recording of isometric contractions *in vitro*

Freshly obtained ileum segments were placed in a dissecting dish containing iced, carbonated Kreb's solution. Segments were opened along the mesenteric border, cleaned, and pinned flat. The mucosal layer was removed and the *muscularis externa* (ME) was cut into strips (5 mm × 15 mm). Strips were mounted along the longitudinal muscle orientation in individual chambers of a vertical organ bath filled with 2.5 ml carbonated Kreb's solution at 37°C. The muscle activity was measured using an isometric force transducer/amplifier (Harvard Apparatus) and recorded on a multi-recorder (Harvard Apparatus) for digital analysis. Muscle strips were equilibrated in the organ bath under 60 mN tension for 60 min at 37°C before they were tested for

contractility. Thereafter, muscle strips were stretched until their optimal length-tension relationship was reached (3). Receptor-mediated and receptor-independent contractile responses were evoked by increasing concentrations of the muscarinic agonist carbachol (CCh, 10-9 to 10-4 M, Sigma-Aldrich) and by KCl (60 mM) respectively. Neurally mediated responses were elicited by pulse trains of electrical field stimulation (EFS, 0.5 – 16 Hz, pulse duration 0.3 ms, train 10 s). Electrical stimuli were generated by a Grass-88 stimulator (Grass). The voltage was kept at 8 V by use of a Med Lab Stimu-Splitter II (Med Lab). Data was acquired and stored using the Windaq Data Acquisition system and a DI-2000 PGH card (Dataq Instruments). Dedicated software (LabChart7, AD Instruments Inc.) was used to process traces and quantify contractile activity. Contractile activity was expressed as mN/mm-2 with mm2 reflecting cross-sectional area (CSA) (4) that was calculated by the following equation after measuring weight and length of each muscle strip at the end of each experiment: CSA (mm2) = tissue weight (mg)/ tissue length (mm) x tissue density (mg mm-3). Tissue density was defined as 1.05 mg mm-3. Contractile responses to EFS are also expressed as % of maximal response to KCl.

Bone Marrow chimera mice generation

For bone marrow cells transplantation, CD45.2 WT and CD45.2 Ccr2-/- recipient mice were irradiated with 9.5 Gy by using a Clinac 2100C Linear Accelerator (Varian Medical Systems). Twenty-four hours after irradiation, 5 x 106 mononuclear cells isolated from bone marrow of CD45.1 wild type (B6.SJL-Ptprca Pepcb/BoyJ) mice by using HISTOPAQUE 1083 (Sigma-Aldrich) were injected via tail vein. Animals were rested for 8 weeks before experiments and bone marrow reconstitution was confirmed by flow cytometry.

Immunofluorescence staining and analysis

Segments of jejunum were isolated and whole mounts were prepared after removal of the mucosa and submucosa in order to obtain preparations of circular and longitudinal smooth muscle

layer and adherent myenteric plexus. Next, preparations were fixed in 4% paraformaldehyde for 30 min at room temperature (RT). After washing with PBS, tissues were stored in PBS containing 0.03% sodium azide until usage. For immune-labeling experiments, tissues were pre-incubated in blocking solution (PBS with 0.5 % Triton X-100 that contained 4% normal serum from the species of the secondary antibodies and 0.01% sodium azide) for 1 hour to reduce nonspecific binding and to permeabilize the tissues. All primary and secondary antibodies were diluted in blocking solution. Subsequently, the whole-mounts were incubated with primary antibodies rat anti-F4/80 (Biolegend); rabbit anti-neurofilament 200 kD (NF200, Abcam); rabbit anti-nNOS C-terminal (Santa Cruz Biotechnology); goat anti-ChAT (Millipore); human ANNA-1 serum anti-HuC/D (5)(kindly provided by Prof. Lennon V. A. Mayo Clinic, Rochester, Minnesota, USA). After washing in PBS, the ME whole-mounts were incubated for 2 hours in a mixture of fluorescently-labeled secondary antibodies (AMCA-conjugated donkey anti-rabbit (Jackson ImmunoLabs); Cy3-conjugated donkey anti-goat (Jackson ImmunoLabs); Alexa 647-conjugated donkey anti-human (ImTec Diagnostic NV); Cy5-conjugated donkey anti-rat (Jackson ImmunoLabs); Cy3-conjugated donkey anti-rabbit(Jackson ImmunoLabs)). In some experiments nuclear staining was performed using DAPI (4',6-Diamidine-2'-phenylindole dihydrochloride; Sigma-Aldrich). Finally, samples were rinsed in PBS, mounted in SlowFade Diamond Antifade mountant (Invitrogen).

Immunofluorescence stainings were visualized using a Zeiss LSM780 confocal laser scanning microscope (Cell Imaging Core, KU Leuven). For each field of view, a z-series spanning the entire depth of the myneteric plexus was imaged and projected for cell counting. In each field the number of ganglia and the number of HuC/D immunoreactive neuronal bodies were counted. The intensity of staining obtained with anti-ChAT and anti-nNOS antibodies was measured using Image J software. Identical acquisition exposure time conditions were used to analyze each image. Corrected total ganglion (ChAT) and image fluorescence (nNOS) was calculated as follows: CTCF = Integrated Density – (Area of selected ganglion X Mean fluorescence of background readings) (6;7).

For the quantification of HuC/D translocation into the nuclei of myenteric neurons, the Imaris software package was used (Bitplane, version 7.6). Z-stacks of confocal images were collected using three channels (DAPI, HuC/D and NF200), spanning the entire volume of HuC/D positive cells. To quantify HuC/D immunoreactivity in the nucleus, surface reconstructions of the DAPI filled nuclei were first set as a mask to isolate overlapping HuC/D and DAPI immunoreactivity. To distinguish between background and cell fill, manually set intensity thresholds were used. The overlapping area of the reconstructed nuclear surface mask (HuC/D with DAPI) was analyzed to define the fluorescence intensity and the volume of HuC/D in the nuclei for individual neurons. Cells were selected for analysis only if the entire cell nucleus was clearly defined and distinguishable within the image (x, y, and z); cells with overlapping nuclei or multinucleated cells were excluded. All images were acquired and analyzed by researchers (G.M and P.J.G-P) blinded to the mouse genotype.

CSF1-Fc treatment

CSF1-Fc was made as previously described (8) and provided by Zoetis (Kalamazoo). The treatment group received 0.75 µg/g CSF1-Fc as previously used in a liver injury model (control: phosphate-buffered saline) (9). CSF1-Fc or saline was administered subcutaneously 24 hours and 1 hour before IM and any following day until sacrifice.

Isolation and digestion of intestinal *muscularis externa*

Full thickness ME from the small intestine was enzymatically digested in MEMα medium (Lonza, Verviers, Belgium) containing 100 µg/ml of Penicillin, 100 µg/ml of Streptomycin, 50 µM beta-mercaptoethanol, 5% fetal calf serum, 5mg/ml protease type I (Sigma-Aldrich), 20 mg/ml collagenase type II (Sigma-Aldrich) and 5U/ml DNase I (Sigma-Aldrich) for 15 minutes at 37 °C. Cell suspensions were filtered through a nylon mesh, centrifuged and stained for flow cytometry.

Flow cytometry

Before staining, single-cell suspensions were pre-incubated with dead cell dye Zombie Aqua (Zombie Aqua Fixable Viability Kit, BioLegend) for 15 min at RT followed by an anti-FcR antibody (clone 2.4G2; BD Biosciences,) to minimise unspecific antibody binding. For surface staining, the following antibodies were used: CD45.2-APC-efluor780 (104, eBioscience), CD11b-PeCy7 (M1/70, BD Biosciences), CD64-Alexa Fluor 647 (X54-5/7.1, BD Biosciences), Ly6G-PercPCy5.5 (1A8, BD Biosciences), Ly6C-PE (AL-21, BD Biosciences), MHCII -FITC (IA/E, M5/114.15.2, eBioscience). Samples were acquired using a FACSCanto (BD Biosciences) and analysed with FlowJo software (version 4.6.2, Treestar).

Cell sorting

Single-cell suspensions of viable cells were stained for the surface markers as indicated above. Before surface staining, cells were incubated with dead cell dye Zombie Aqua (1:1000, Zombie Aqua Fixable Viability Kit, BioLegend) for 15 min at RT. Cells were sorted by fluorescence-activated cell sorting (FACS) (FACSAria; BD Biosciences) into Ly6C+MHCII-, Ly6C+MHCII+, Ly6C-MHCIIlo and Ly6C-MHCIIhi populations gated on the Zombie Aqua- CD45.2+CD11b+Ly6G- cells.

In vitro stimulation and intracellular cytokine detection

For ex vivo cytokine detection, single-cell suspensions were cultured at 5×10^5–1×10^6 cells per well in 96-well round-bottom plates in RPMI 1640 (Lonza) supplemented with 10% fetal bovine serum (Gibco, Invitrogen, Life technologies), 1% penicillin streptomycin (Gibco, Invitrogen, Life technologies), glutamine (Gibco, Invitrogen, Life technologies), nonessential amino acids (Lonza) and 50 mM of β-mercaptoethanol (Invitrogen, Life technologies) in presence of 1µl/ml brefeldin A (GolgiPlug, BD Biosciences). After 3 hours, cells were surface stained as described above, then washed twice with FACS buffer, fixed for 30 min and permeabilized for 20 min (FoxP3 intracellular staining kit, eBioscience). Cells were then incubated for intracellular staining with the following

antibodies: TNF-α-APC (MP6-XT22, eBioscience), IL-6-PE (MP5-20F3, eBioscience) or isotype control antibodies rat IgG1, rat IgG2b (eBioscience).

Detection of reactive oxygen species in neutrophils

Single-cell suspensions were plated at 1×10^6 cells per well, in 96-well round-bottom plates and re-suspended in complete medium containing 2 ng/ml dihydrorhodamine 123 (Invitrogen). Cells were incubated for 30 min at 37 °C and then washed with FACS buffer before being stained for the surface markers as described above.

In vivo proliferation assays

Proliferation was assessed via Bromodeoxyuridine incorporation or Ki67 expression. Mice were given an intraperitoneal injection of 1 mg Bromodeoxyuridine (Sigma-Aldrich) 2 hours before sacrifice. ME from the small intestine was isolated and digested enzymatically as described above. Cell proliferation was assessed by flow cytometry using BrdU intracellular staining following the manufacturer's instructions (BrdU flow Kits, BD Biosciences). Expression of Ki67 was evaluated via Ki67-Alexa Fluor 647 (B56, BD Biosciences) intracellular staining. Before incubation with Ki67 antibody, cells were surface stained, fixed and permeabilized as described above.

Monocyte isolation and adoptive transfer

Murine bone marrow cells were obtained from femur and tibias of UBI-GFP (C57BL/6-Tg(UBC-GFP)30Scha/J) mice by flushing the shaft with PBS using a syringe and a 26G needle and passed through 30 µm nylon mesh. Monocytes were isolated from the bone marrow by depletion of non-target cells according to the manufacturer's instructions (Monocyte Isolation Kit BM, MACS, Miltenyi Biotec). After isolation, 2×10^6 monocytes were injected into the tail vein of recipient mice.

Masson's trichrome staining and quantification of fibrosis

Segments of small intestine were fixed with zinc formaldehyde for 48 hours, kept in 70% ethanol for 48 hours and embedded in paraffin. Horizontal cross sections were rehydrated and stained for Masson's trichrome staining following manufacturer's instructions (Accustain Trichrome Stains Masson, Sigma-Aldrich). Images were acquired with a BX41 microscope (Olympus) using a SC30 camera (Olympus) and visualized using Cell^F software (Olympus). Images were taken with a 10X objective (655.4 µm x 490.1 µm) by a researcher blinded to the sample coding (G.M). Ten randomly chosen sections were analyzed per mouse by a researcher blinded to the sample coding (G.F.). Thickness of the ME and serosa was calculated as mean value of 10 different points per section using ImageJ 1.45 software (U. S. National Institutes of Health, Bethesda, Maryland, USA). The level of blue was quantified via a threshold color method using ImageJ 1.45 software (U. S. National Institutes of Health, Bethesda, Maryland, USA) and expressed as % of blue area over total area of the section. The percentage of blue area was used as an indication for the deposition of collagen.

RNA extraction and gene expression

Full thickness ME from the small intestine was preserved in RNA Later for 24 hours. Tissue was homogenized by the TissueLyser II homogenizer (Qiagen). RNA extraction was performed using RNeasy Mini Kit (Qiagen) following manufacturer's instructions. Total RNA was transcribed into complementary DNA (cDNA) by qScript cDNA SuperMix (Quanta Biosciences) according to the manufacturer's instructions. Quantitative real-time transcription polymerase chain reactions (RT-PCR) were performed with the LightCycler 480 SYBR Green I Master (Roche) on the Light Cycler 480 (Roche). Results were quantified using the 2-ΔΔCT method (10). Expression levels of the genes of interest were normalized to the expression levels of the reference gene Rpl32. Gene expression levels are shown as fold change versus gene expression in naïve control tissues or normalized to reference gene Rpl32 in the case of sorted cells. Quantitative-PCR experiments were performed in triplicate and results are expressed as mean values. Primer sequences used are listed in table 1.

Table 1. Primer sequences used for quantitative RT-PCR.

Gene	Sense	Antisense
rpl32	5'-AAGCGAAACTGGCGGAAAC-3'	5'-TAACCGATGTTGGGCATCAG-3'
il6	5'-CCATAGCTACCTGGAGTACATG-3'	5'-TGGAAATTGGGGTAGGAAGGAC-3'
il1a	5'-GAGAGCCGGGTGACAGTATC-3'	5'-ACTTCTGCCTGACGAGCTTC-3'
il1b	5'-GACCTTCCAGGATGAGGACA-3'	5'-TCCATTGAGGTGGAGAGCTT-3'
tnfa	5'-TCTTCTCATTCCTGCTTGTGG-3'	5'-CACTTGGTGGTTTGCTACGA-3'
cxcl1	5'-GCTGGGATTCACCTCAAGAA-3'	5'-TCTCCGTTACTTGGGGACAC-3'
ccl2	5'-CACGTGTTGGCTCAGCCAGATGC-3'	5'-CCTTCTTGGGGTCAGCACAGACC-3'
cxcl2	5'-AATGCCTGAAGACCCTGCCAAG-3'	5'-CTCCTTTCCAGGTCAGTTAGCC-3'
il4ra	5'-GCAGATGGCTCATGTCTGAA-3'	5'-CTCTGGGAAGCTGGGTGTAG-3'
mrc1	5'-GCAAATGGAGCCGTCTGTGC-3'	5'-CTCGTGGATCTCCGTGACAC-3'
ym1	5'-GGGCATACCTTTATCCTGAG-3'	5'-CCACTGAAGTCATCCATGTC-3'
lyve1	5'-CTGGCTGTTTGCTACGTGAA-3'	5'-CATGAAACTTGCCTCGTGTG-3'
stab1	5'-ACGGGAAACTGCTTGATGTC-3'	5'-ACTCAGCGTCATGTTGTCCA-3'
arg1	5'-TCACCTGAGCTTTGATGTCG-3'	5'-TTATGGTTACCCTCCCGTTG-3'
vegfa	5'-CAGGCTGCTGTAACGATGAA-3'	5'-AATGCTTTCTCCGCTCTGAA-3'
cd163	5'-GAGCATGAATGAAGTGTCCG-3'	5'-CAGGCTGCTGTAACGATGAA-3'

Supplementary figures

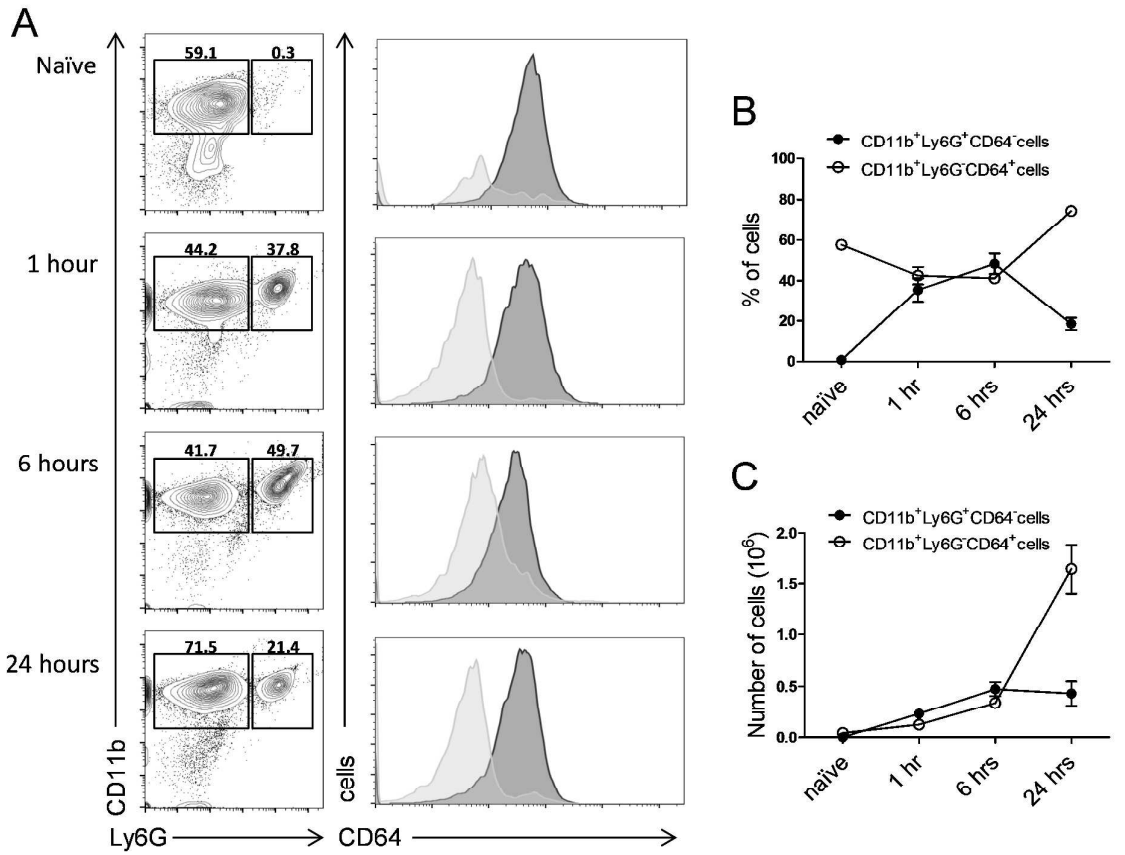

Supplementary figure 1. Intestinal manipulation induces influx of leukocytes into the *muscularis externa*. Infiltration of immune cells into the ME of naïve mice and 1, 6 and 24 hrs after IM was assessed via flow cytometry. (A) Representative dot plot showing $CD11b^{+}Ly6G^{+}CD64^{-}$ and $CD11b^{+}Ly6G^{-}CD64^{+}$ cells gated on the $CD45^{+}$ immune cells. Histograms showed expression level of CD64 on cells in gate R1 and R2. (B) Percentages of $CD11b^{+}Ly6G^{+}CD64^{-}$ (neutrophils) and $CD11b^{+}Ly6G^{-}CD64^{+}$ cells (monocytes and macrophages). (C) Absolute numbers of $CD11b^{+}Ly6G^{+}CD64^{-}$ and $CD11b^{+}Ly6G^{-}CD64^{+}$ cells. Each data set included 6 mice.

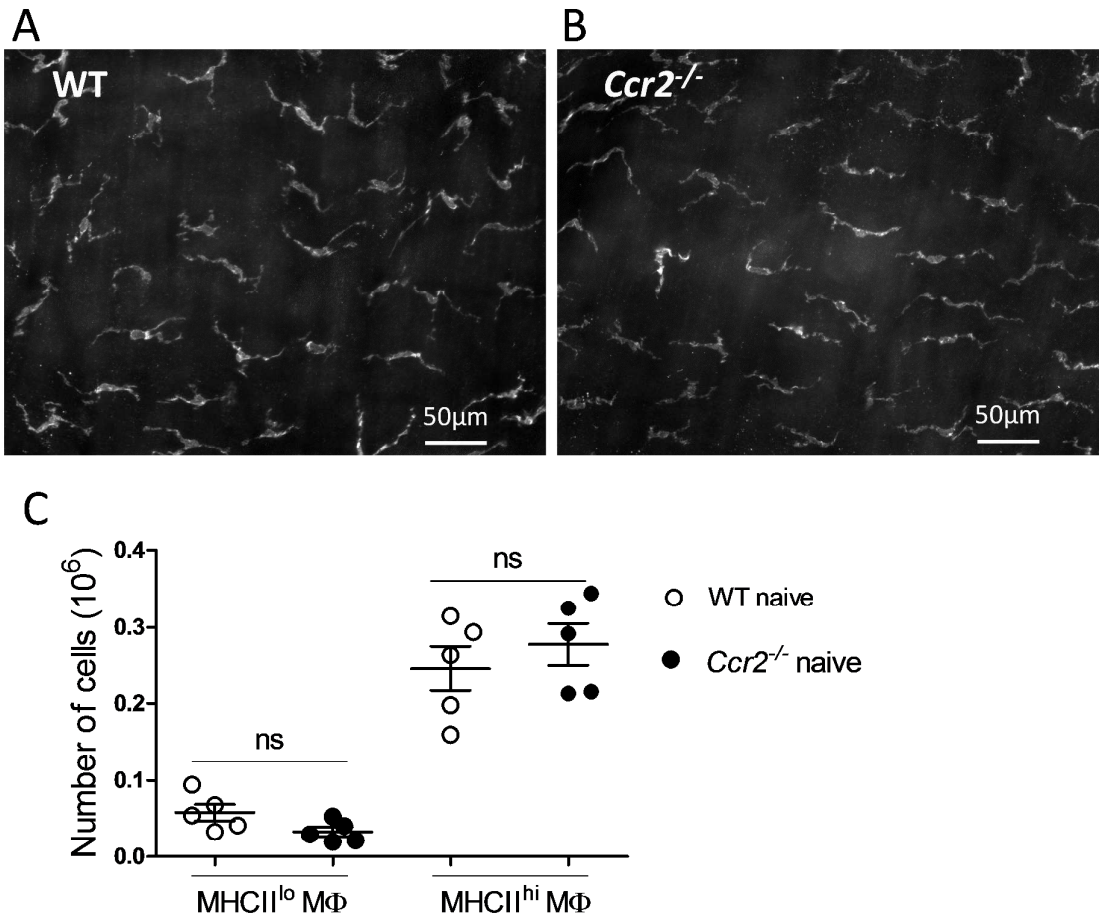

Supplementary figure 2. *Ccr2*$^{-/-}$ and WT mice have similar morphology, distribution and number of resident *muscularis externa* macrophages. (A) F4/80+ MΦs in naïve ME of WT mice. (B) F4/80+ MΦs in naïve ME of Ccr2$^{-/-}$ mice. (C) Absolute numbers of CD45^{+}CD11b^{+}Ly6G^{-}Ly6C^{-}MHCII^{lo} and CD45^{+}CD11b^{+}Ly6G^{-}Ly6^{C-}MHCII^{hi} MΦs in naïve WT (white dots) and naïve Ccr2$^{-/-}$ mice (black dots) obtained by flow cytometry analysis. WT and Ccr2$^{-/-}$ data sets were determined via unpaired t-test (ns= not significant).

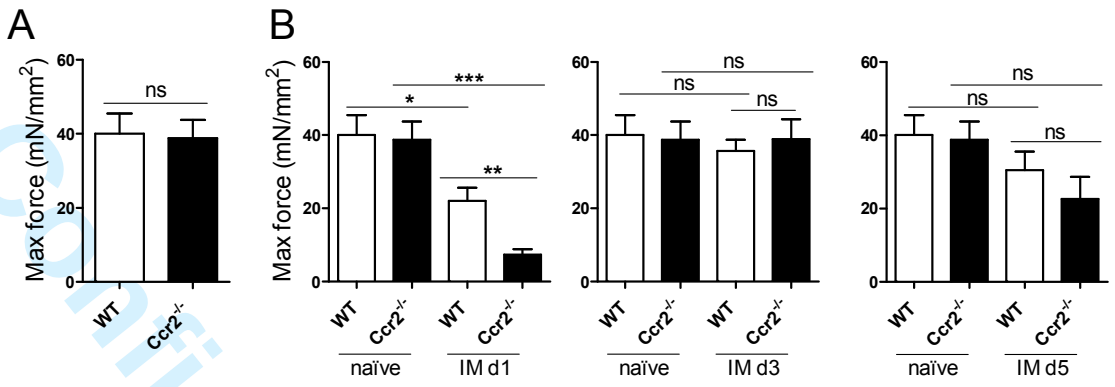

Supplementary figure 3. Depolarizing high potassium chloride solution (KCl)-induced muscle contractions are severely affected in Ccr2$^{-/-}$ mice at day 1 after IM. Ileal longitudinal smooth muscle strips from naïve WT and Ccr2$^{-/-}$ mice and 1, 3 and 5 days after IM were stimulated in vitro with high potassium solution (KCl 60 mM). (A) Contractile responses recorded in strips isolated from naïve WT and Ccr2$^{-/-}$ mice were compared via unpaired t-test. (B) Contractile responses recorded in strips isolated 1, 3 and 5 days after IM were compared with responses recorded in naïve control data sets via unpaired t-test. (* $P < 0.05$, ** $P < 0.01$, *** $P < 0.001$, ns= not significant).

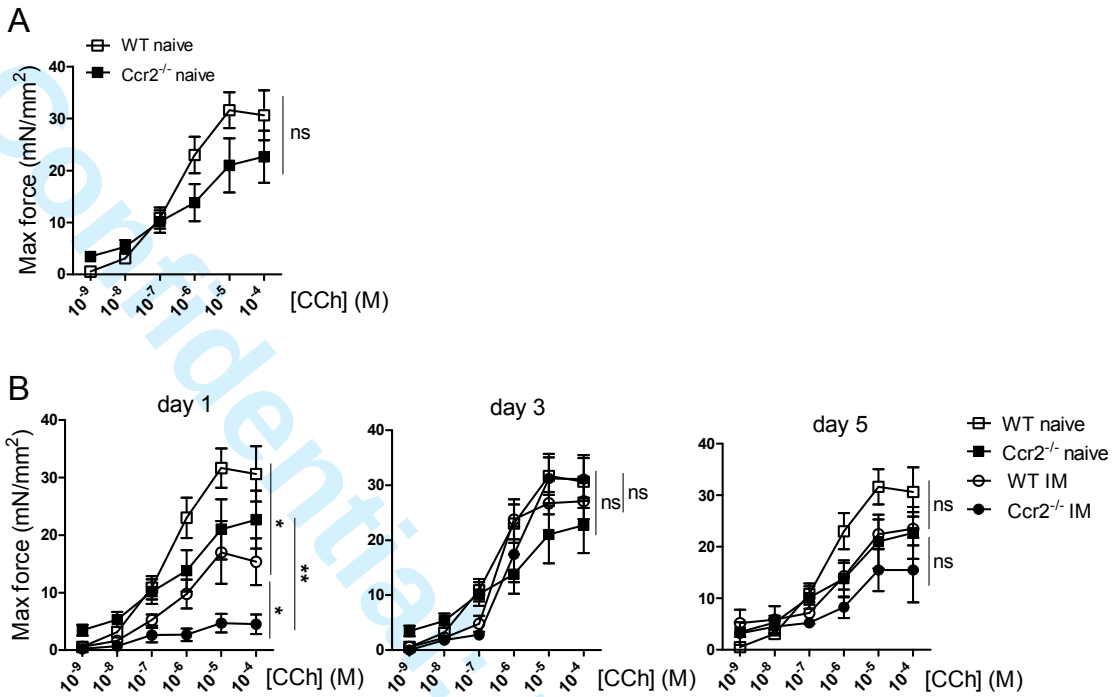

Supplementary figure 4. Carbachol (CCh)-induced muscle contractions are severely affected in Ccr2-/- mice compared to WT mice at 1 day after IM. Ileal longitudinal smooth muscle strips were isolated from naïve WT and Ccr2$^{-/-}$ mice and 1, 3 and 5 days after IM and stimulated in vitro with increasing concentrations of carbachol. (A) Contractile responses recorded in strips isolated from naïve WT and Ccr2$^{-/-}$ mice were compared via two-way ANOVA test followed by Bonferroni correction. (B) Contractile responses recorded in strips isolated 1, 3 and 5 days after IM were compared with responses recorded in the naïve control data sets via two-way ANOVA test followed by Bonferroni correction (* $P < 0.05$, ** $P < 0.001$ and ns= not significant).

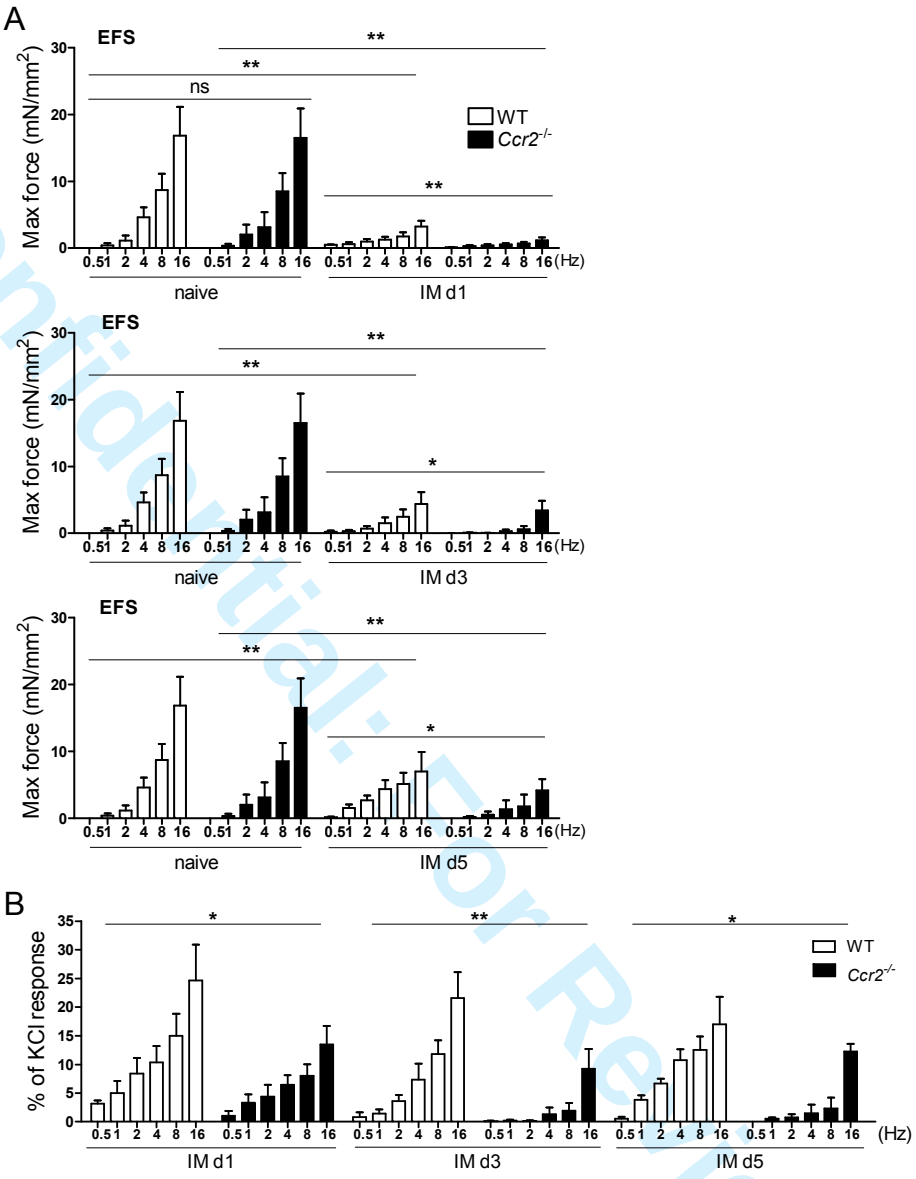

Supplementary figure 5. Electrical field stimulation (EFS)-induced muscle contractions are severely impaired by IM in Ccr2$^{-/-}$ mice. Ileal longitudinal smooth muscle strips isolated from naïve WT and Ccr2$^{-/-}$ mice and 1, 3 and 5 days after IM were stimulated in vitro with EFS at increasing frequencies. (A) Contractile responses recorded in strips isolated from naïve WT and Ccr2$^{-/-}$ mice or after 1, 3 and 5 days after IM were compared via two-way ANOVA test followed by Bonferroni correction (* $P < 0.05$ and ** $P < 0.001$ and ns= not significant). (C) Contractile responses to EFS were normalized to contractile responses to KCl (60mM) and expressed as percentages. WT and Ccr2$^{-/-}$ data sets were compared at each time point and statistical significance calculated via two-way ANOVA test followed by Bonferroni correction (* $P < 0.05$ and ** $P < 0.001$).

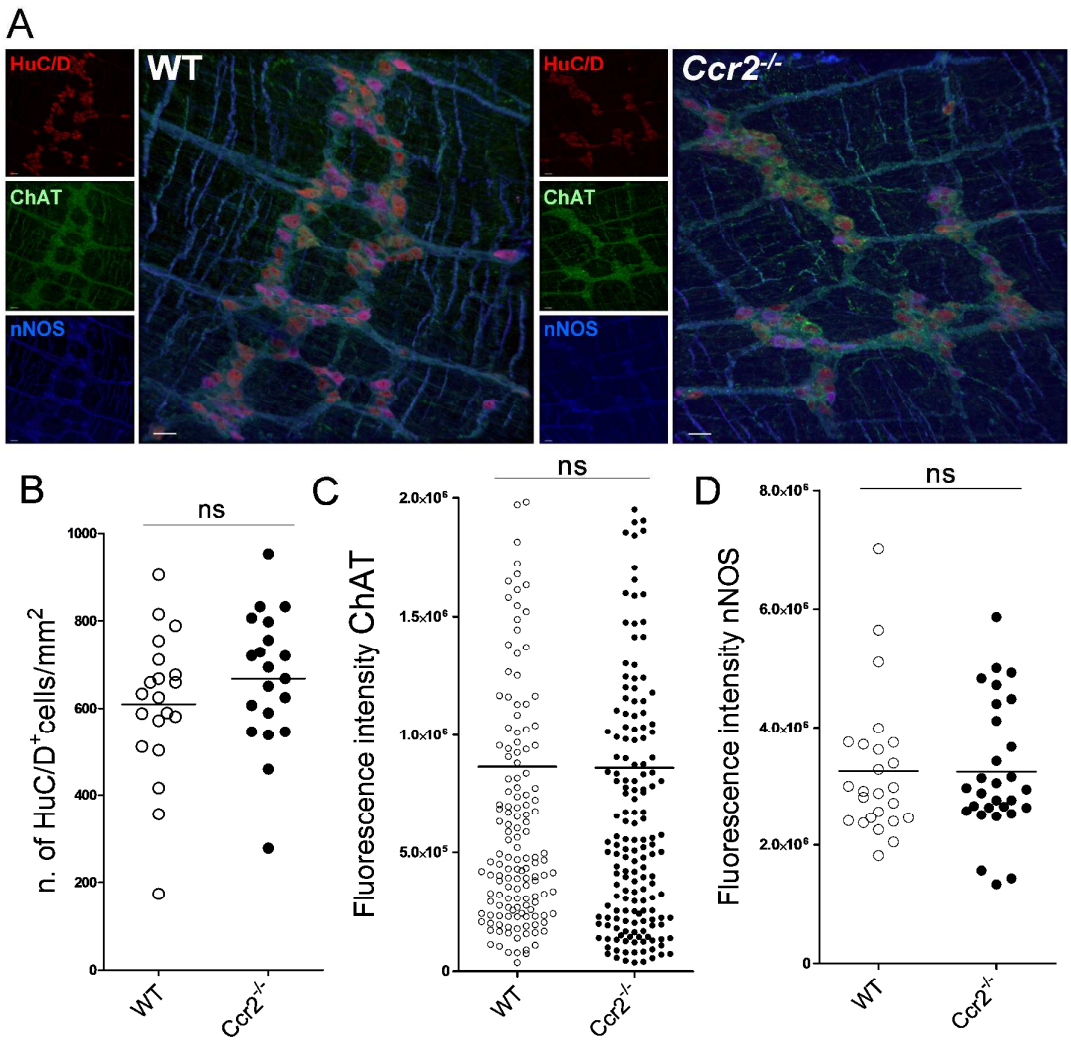

Supplementary figure 6. Lack of CCR2-monocytes does not reduce number of myenteric neurons and ChAT and nNOS expression after intestinal manipulation. (A) Representative immune-fluorescent labelling of whole mount preparations of ME isolated 5 days after IM from WT and Ccr2$^{-/-}$ mice. Neuronal cell bodies are identified via HuC/D, ChAT and nNOS and were respectively used as markers of cholinergic and nitrergic neurons, scale bar is 20µm. (B) Numbers of HuC/D^{+} cells per mm2 counted in 4 randomly chosen fields per animal. Each dot represents data from an individual field and mean ± SEM are shown for both groups. Statistical significance was determined by t-test; ns = not significant. (C) The intensity of stainings obtained with anti-ChAT antibody and with (D) anti-nNOS were measured. Data are shown as corrected fluorescence value. WT and Ccr2$^{-/-}$ data sets were compared via unpaired t-test (ns = not significant).

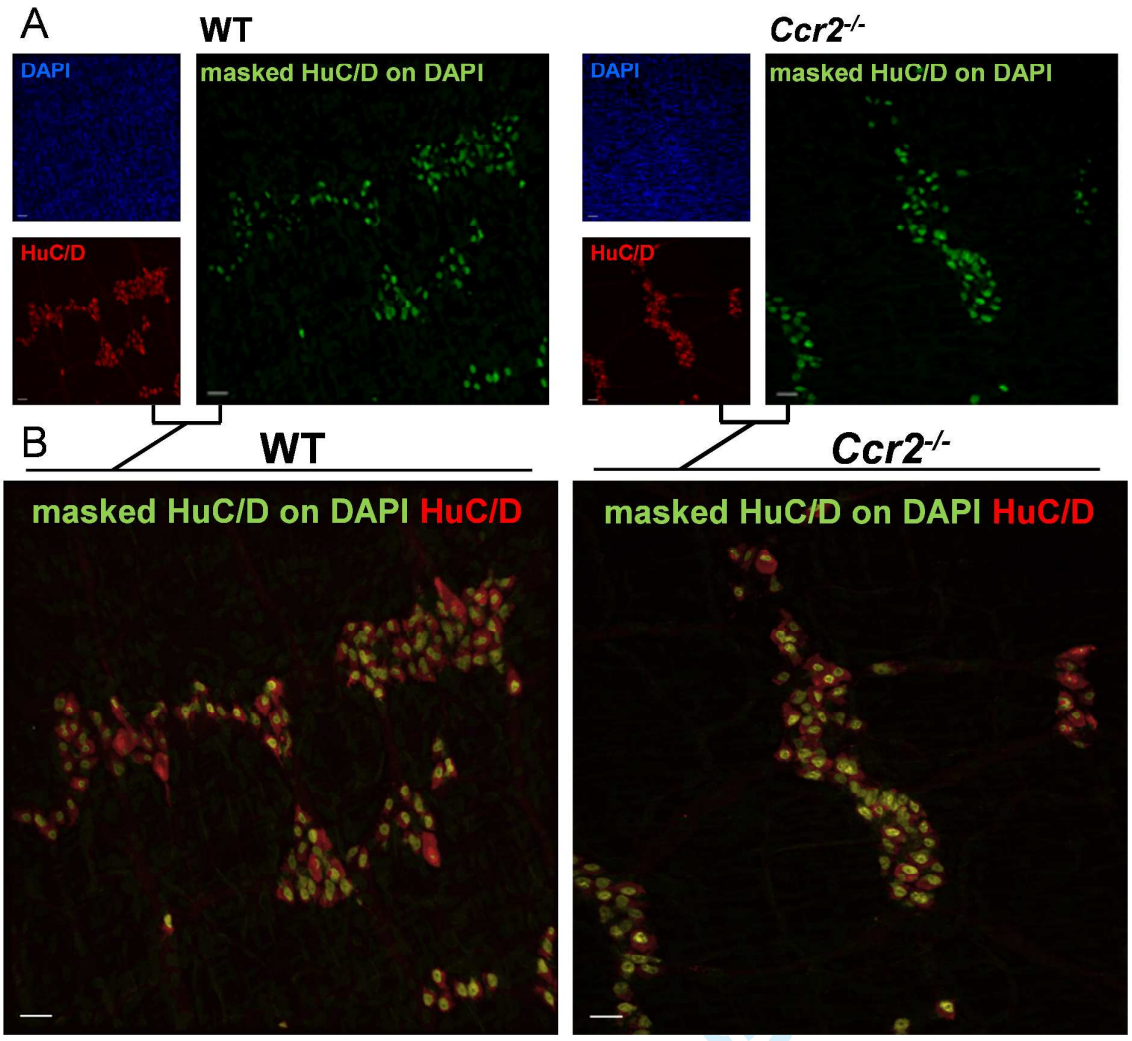

Supplementary figure 7. Lack of CCR2-monocytes increases HuC/D translocation to the nuclei of enteric neurons. (A) Representative images of whole mount preparations of ME isolated 5 days after IM from WT and Ccr2$^{-/-}$ mice. Neuronal cell bodies are identified via HuC/D (red) and nuclei with DAPI (blue). The overlapping area of the reconstructed nuclear surface mask of HuC/D immunoreactivity within DAPI signal is shown in green, scale bar is 20µm. (B) Representative images showing the masked HuC/D in DAPI over the total HuC/D signal.

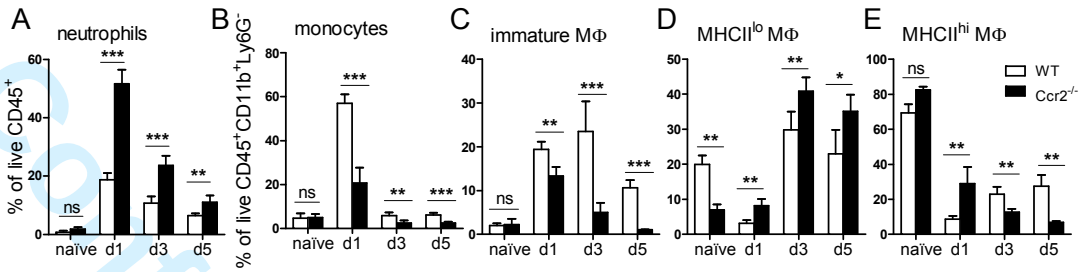

Supplementary figure 8. Percentages of leucocytes accumulating into the *muscularis externa* at different time points after intestinal manipulation. Immune cells isolated from the ME of naïve WT and *Ccr2*$^{-/-}$ mice and 1, 3 and 5 days after IM were analyzed via flow cytometry. Percentages of CD11b^{+}Ly6G^{+} neutrophils (A), Ly6C^{hi}MHCII^{-} monocytes (B), Ly6C^{+}MHCII^{+} immature MΦ (C), Ly6C^{-} MHCII^{lo} (D) and Ly6C^{-}MHCII^{hi} MΦ (E) in WT (white bars) and *Ccr2*$^{-/-}$ mice (black bars). Statistical significance between WT and *Ccr2*$^{-/-}$ data sets was determined via unpaired t-test (* $P < 0.05$, ** $P < 0.001$, *** $P < 0.0001$ and ns= not significant).

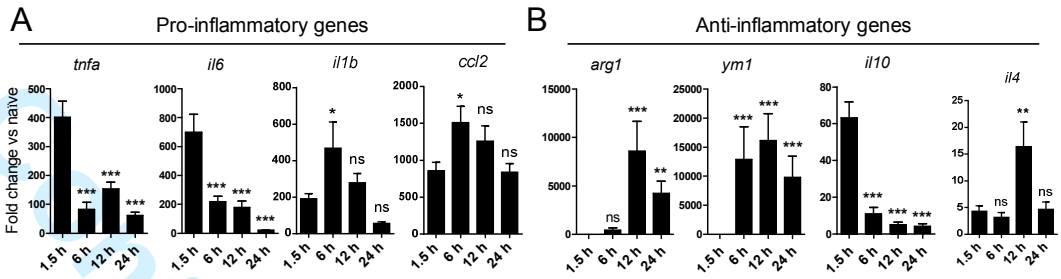

Supplementary figure 9. Expression of pro-inflammatory and anti-inflammatory genes during the acute phase after IM. Gene expression levels of pro-inflammatory genes and anti-inflammatory genes were measured in homogenates of ME of WT mice at different time points after IM. Fold change over naïve WT mice mean values ± SEM of mRNA levels of pro (A) and anti-inflammatory genes (B). All data sets were compared to gene expression at 1.5h via one-way ANOVA followed by Dunnett's Multiple Comparison Test (* $P < 0.05$, *** $P < 0.0001$ and ns= not significant).

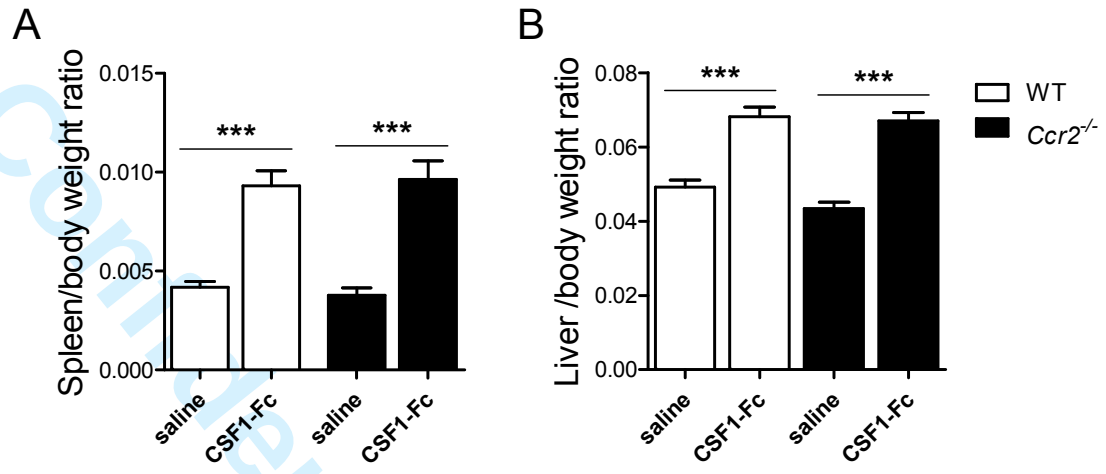

Supplementary Figure 10. CSF1-Fc treatment increases spleen and liver weight. Spleen (A) and liver (B) weight ratio over body weight of WT and *Ccr2*$^{-/-}$ mice treated with (0.75 µg/g) CSF1 Fc or saline for 4 consecutive days. Statistical significance between CSF1-Fc and saline-treated data sets was determined via unpaired t-test (*** $P < 0.0001$).

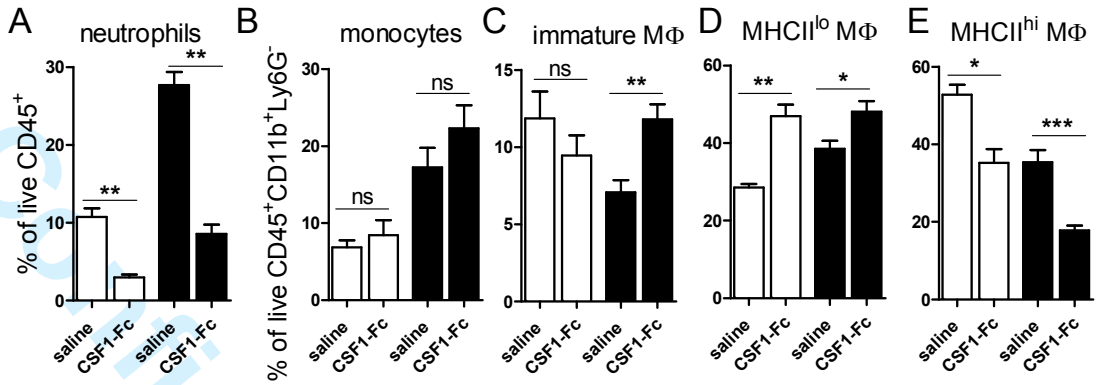

Supplementary Figure 11. CSF1 reduces influx of neutrophils and drives accumulation of macrophages into the *muscularis externa* during recovery after IM. WT and Ccr2$^{-/-}$ mice undergoing IM were treated with either CSF1-Fc or saline. Percentages of CD11b^{+}Ly6G^{+} neutrophils (A), Ly6C^{hi}MHCII^{-} monocytes (B), Ly6C^{+}MHCII^{+} immature MΦ (C), Ly6C^{-}MHCII^{lo} (D) and Ly6C^{-}MHCII^{hi} MΦ (E) in WT and *Ccr2*$^{-/-}$ mice 3 days after IM. Statistical significance between CSF1-Fc and saline-treated data sets was determined via unpaired t-test (* $P < 0.05$, ** $P < 0.001$, *** $P < 0.0001$ and ns= not significant).

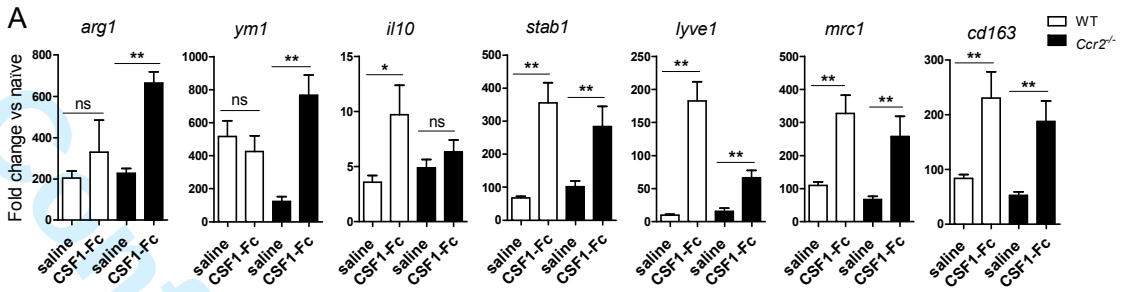

Supplementary Figure 12. CSF1-Fc treatment drives expression of anti-inflammatory genes in the *muscularis externa* during recovery. Gene expression levels of anti-inflammatory gens were measured in homogenates of ME from WT and Ccr2$^{-/-}$ mice treated with either CSF1-Fc or saline 3 days after IM. (A) mRNA levels are expressed as fold change mean values ± SEM versus naïve. Statistical significance between CSF1-Fc and saline-treated data sets was determined via unpaired t-test (* $P < 0.05$, ** $P < 0.001$ and ns= not significant).

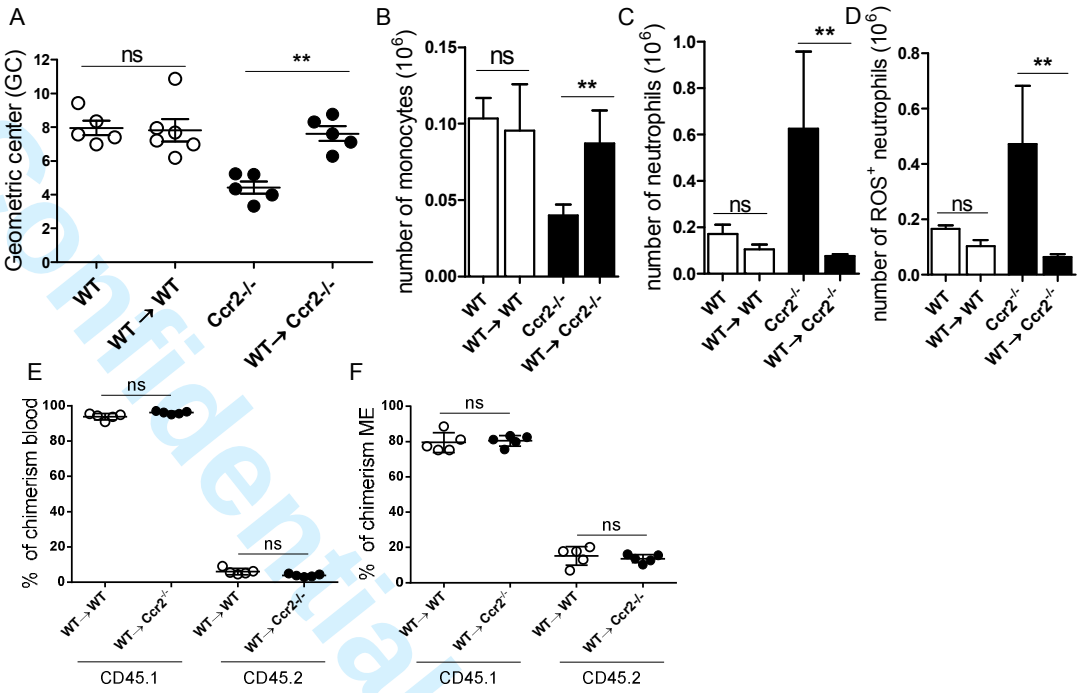

Supplementary Figure 13. Wild type bone marrow transplantation in CCR2-deficient mice results in recovery of gastrointestinal transit with normalization of monocytes and neutrophils recruitment after intestinal manipulation. Irradiated CD45.2 Ccr2$^{-/-}$ and WT mice were reconstituted with CD45.1 wild type bone marrow-derived cells to generate WT →Ccr2$^{-/-}$ and WT →WT mice. After reconstitution chimera mice were subjected to intestinal manipulation and gastrointestinal transit and immune cells recruited at the muscularis externa evaluated 3 days after. (A) GC values of dextran distribution through the intestinal segments in the indicated mouse groups. Number of monocytes (B), neutrophils (C) and ROS-positive neutrophils (D) in the muscularis externa of the small intestine 3 days after IM is shown. Percentage of chimerism was evaluated via flow cytometry calculating the amount of CD45.2 versus CD45.1 in blood and ME in WT →Ccr2$^{-/-}$ and WT →WT mice. Statistical significance between Ccr2$^{-/-}$ and WT →Ccr2$^{-/-}$ data sets was determined via unpaired t-test (** $P < 0.001$ and ns= not significant).

Reference List

(1) Gomez-Pinilla PJ, Farro G, Di GM *et al*. Mast cells play no role in the pathogenesis of postoperative ileus induced by intestinal manipulation. *PLoS One* 2014;**9**(1):e85304.

(2) Sikkink CJ, de MB, Bleichrodt RP *et al*. Auto-cross-linked hyaluronic acid gel does not reduce intra-abdominal adhesions or abscess formation in a rat model of peritonitis. *J Surg Res* 2006;**136**(2):255-9.

(3) Pelckmans PA, Boeckxstaens GE, Van Maercke YM *et al*. Acetylcholine is an indirect inhibitory transmitter in the canine ileocolonic junction. *Eur J Pharmacol* 1989;**170**(3):235-42.

(4) Moreels TG, De Man JG, De Winter BY *et al*. How to express pharmacological contractions of the inflamed rat intestine. *Naunyn Schmiedebergs Arch Pharmacol* 2001;**364**(6):524-33.

(5) Lennon VA, Sas DF, Busk MF *et al*. Enteric neuronal autoantibodies in pseudoobstruction with small-cell lung carcinoma. *Gastroenterology* 1991;**100**(1):137-42.

(6) Burgess A, Vigneron S, Brioudes E *et al*. Loss of human Greatwall results in G2 arrest and multiple mitotic defects due to deregulation of the cyclin B-Cdc2/PP2A balance. *Proc Natl Acad Sci U S A* 2010;**107**(28):12564-9.

(7) Potapova TA, Sivakumar S, Flynn JN *et al*. Mitotic progression becomes irreversible in prometaphase and collapses when Wee1 and Cdc25 are inhibited. *Mol Biol Cell* 2011;**22**(8):1191-206.

(8) Gow DJ, Sauter KA, Pridans C *et al*. Characterisation of a novel Fc conjugate of macrophage colony-stimulating factor. *Mol Ther* 2014;**22**(9):1580-92.

(9) Stutchfield BM, Antoine DJ, Mackinnon AC *et al*. CSF1 Restores Innate Immunity After Liver Injury in Mice and Serum Levels Indicate Outcomes of Patients With Acute Liver Failure. *Gastroenterology* 2015;**149**(7):1896-909.

(10) Livak KJ, Schmittgen TD. Analysis of relative gene expression data using real-time quantitative PCR and the 2(-Delta Delta C(T)) Method. *Methods* 2001;**25**(4):402-8.

Title page:

CCR2-dependent monocyte-derived macrophages resolve inflammation and restore gut motility in postoperative ileus.

Short title: Macrophages resolve postoperative ileus

Giovanna Farro[1], Michelle Stakenborg[1], Pedro J Gomez-Pinilla[1], Evelien Labeeuw[1], Gera Goverse[1], Martina Di Giovangiulio[1], Nathalie Stakenborg[1], Elisa Meroni[1], Francesca D'Errico[1], Yvon Elkrim[2,3], Damya Laoui[2,3], Zofia M. Lisowski[4], Kristin A. Sauter[4], David A. Hume[4], Jo A. Van Ginderachter[2,3], Guy E. Boeckxstaens[1#] & Gianluca Matteoli[1#].

[1]KU Leuven Department of Clinical and Experimental Medicine, Translational Research Center for Gastrointestinal Disorders (TARGID), Leuven, Belgium. [2]Myeloid Cell Immunology Lab, VIB Inflammation Research Center, Ghent, Belgium. [3]Lab of Cellular and Molecular Immunology, Vrije Universiteit Brussel, Pleinlaan 2, B-1050 Brussels, Belgium. [4]The Roslin Institute and Royal (Dick) School of Veterinary Studies, University of Edinburgh, Easter Bush, EH25 9RG, UK.

[#] These authors contributed equally as co-last authors.

Corresponding authors:

Prof. Gianluca Matteoli & **Prof. Guy E. Boeckxstaens**
Department of Clinical and Experimental Medicine
Translational Research Center for Gastrointestinal Disorders (TARGID)
KU Leuven; Herestraat 49, O&N1, bus 701; 3000, Leuven, Belgium
Tel: +32-16-330238/ +32-16-345750

E-mail: **gianluca.matteoli@kuleuven.be** and **guy.boeckxstaens@kuleuven.be**

Word count: 4314

Summary 'box':

What is already known about this subject?

- Monocytes and neutrophils infiltrate the *muscularis externa* within a few hours after abdominal surgery
- Infiltration of neutrophils and monocytes after surgery has been correlated to impaired muscle contraction and delayed intestinal transit typical of postoperative ileus

What are the new findings?

- Blocking influx of monocyte migration to the *muscularis externa* after intestinal manipulation does not prevent postoperative ileus
- Lack of monocyte migration to the *muscularis externa* may have dramatic side effects on the recovery of GI transit after open abdominal surgery associated with increased neutrophil-mediated immunopathology and persistent impaired neuromuscular function
- Monocyte-derived macrophages are crucial to the resolution of muscularis inflammation and recovery of gastro-intestinal functions during postoperative ileus

How might it impact on clinical practice in the foreseeable future?

- Our findings imply that inappropriate targeting of the cellular immune response may increase neutrophil-mediated immunopathology and prolong the clinical outcome of POI
- Future therapies should be aimed at enhancing physiological repair functions of macrophages rather than preventing monocyte recruitment to the tissue.

Abstract

Objective. Postoperative ileus (POI) is assumed to result from myeloid cells infiltrating the intestinal *muscularis externa* (ME) in patients undergoing abdominal surgery. In the current study, we investigated the role of infiltrating monocytes in a murine model of intestinal manipulation (IM)-induced POI in order to clarify whether monocytes mediate tissue damage and intestinal dysfunction or they are rather involved in the recovery of intestinal motility. **Design**. IM was performed in mice with defective monocyte migration to tissues (C-C motif chemokine receptor 2, *Ccr2*$^{-/-}$ mice) and wild-type (WT) mice to study the role of monocytes and monocyte-derived macrophages (MΦs) during onset and resolution of ME inflammation. **Results.** At early time points, IM-induced GI transit delay and inflammation were equal in WT and *Ccr2*$^{-/-}$ mice. However, GI transit recovery after IM was significantly delayed in *Ccr2*$^{-/-}$ mice compared to WT mice, associated with increased neutrophil-mediated immunopathology and persistent impaired neuromuscular function. During recovery, monocytes differentiated into MΦs and up-regulated pro-resolving genes. Treatment with MΦ colony-stimulating factor 1 (CSF1) enhanced monocyte recruitment and MΦ differentiation and ameliorated GI transit in *Ccr2*$^{-/-}$ mice. **Conclusion.** Our study reveals a critical role for monocyte-derived MΦs in restoring intestinal homeostasis after surgical trauma. From a therapeutic point of view, our data indicate that inappropriate targeting of monocytes may increase neutrophil-mediated immunopathology and prolong the clinical outcome of POI, while future therapies should be aimed at enhancing MΦ physiological repair functions.

Key words: postoperative ileus; monocytes; monocyte-derived macrophages; colony-stimulating factor 1.

Introduction

Abdominal surgery is often associated with a transient episode of intestinal dysmotility accompanied by symptoms ranging from abdominal pain to constipation and the inability to tolerate a solid diet, referred to as postoperative ileus (POI) (1). Besides the discomfort experienced by patients and possible complications, POI is the most common cause of prolonged hospital stay following abdominal surgery and the annual cost has been estimated as much as $ 1.5 billion in USA, having a large socio-economic impact (2).

POI is a multifactorial condition deriving from many surgery-related factors that contribute to reduce the contractility of the intestinal *muscularis externa* (ME) and to delay GI transit after surgery. For example, the effect of anesthetics, postoperative opioids, inhibitory neural reflexes and inflammatory mediators released by immune cells invading the ME after surgical handling of the intestine have been shown to concur with the development of POI (1).

One of the earliest steps in the inflammatory cascade occurring after abdominal surgery is activation of ME resident macrophages (MΦs), a uniquely adapted population of resident MΦs (3;4). At steady state, ME MΦs respond to luminal bacterial infections and interact with enteric neurons to regulate gastrointestinal motility (5). Once activated, resident MΦs recruit leukocytes, in particular monocytes and neutrophils to the ME, within a few hours after surgery (6). Infiltration of neutrophils and monocytes after surgery has been temporally correlated with impaired muscle contraction and delayed intestinal transit (7). Previous studies have shown that inactivation or depletion of resident MΦs prior to surgery prevented leukocyte recruitment and ameliorated GI transit (7;8). A similar beneficial outcome was obtained by blocking adhesion molecules on the endothelial surface to prevent leukocyte infiltration (6;9;10). However, during inflammation recruitment of leukocytes, and in particular monocytes, is crucial to the timely resolution of the inflammatory process and to prevent excessive tissue damage. In the context of sterile inflammation, while $CCR2^+$ circulating monocytes may initiate pathology, monocyte-derived MΦs typically undergo alternative activation

and acquire a pro-resolving phenotype. Monocyte-derived MΦs have been shown to be critical for repair and functional recovery of various types of organs (11-13), via the release of anti-inflammatory and reparative cytokines and growth factors (14;15). In the context of POI, anti-inflammatory mediators such as the immune-modulatory cytokine IL-10 and poly-unsaturated fatty acids (PUFA)-derived pro-resolving molecules have been shown to be involved in the recovery of intestinal motility (16-18). However, mechanisms of inflammation and resolution have not been fully clarified and the role of monocyte trafficking the ME and MΦ function following surgery remains to be determined.

In the current study, using CCR2-deficient mice (*Ccr2*$^{-/-}$), we investigated the role of infiltrating monocytes in a murine model of IM-induced POI in order to clarify whether monocytes mediate tissue damage and intestinal dysfunction or are rather involved in the recovery of intestinal motility after surgical trauma. In contrast with the current view, our study demonstrates that CCR2-mediated monocyte infiltration does not contribute to the development of surgery-induced POI. Conversely, monocyte-derived MΦs acquire a pro-resolving phenotype and are essential for postoperative recovery. In line, treatment with colony-stimulating factor 1 (CSF1) could overcome CCR2 deficiency and promote monocyte migration to the ME accelerating resolution of inflammation and recovery of GI motility. Our work suggests that future therapies aiming at enhancing MΦ physiological repair functions may represent an ideal approach to accelerate recovery in patients with POI.

Material and Methods

Animals

Twelve week old female wild-type (WT; C57BL/6JOlaHsd), Ccr2 knockout (Ccr2$^{-/-}$; B6.129S4-*Ccr2*^{tm1Ifc}/J), and UBI-GFP (C57BL/6-Tg(UBC-GFP)30Scha/J) mice were kept at the KU Leuven animal facility under SPF conditions on a 12:12-h light-dark cycle and provided with commercially available chow (ssniff® R/M-H, ssniff Spezialdiäten GmbH) and tap water *ad libitum*. All experimental procedures were approved by the Animal Care and Animal Experiments Committee of the University of Leuven (Leuven, Belgium).

Experimental model of POI

An established model of intestinal manipulation (IM) was used to induce POI (19).. A midline laparotomy followed by IM was performed as previously reported (19). During and after the surgical procedure, mice were positioned on a heat pad (32°C) until they recovered from anesthesia. Naïve mice did not undergo any surgical procedure.

Statistical analysis

Significance between two groups was determined by unpaired two-tailed Student's t Test or non-parametric Mann-Whitney test, while one-way analysis of variance (one-way ANOVA) followed by Dunnett's Multiple comparison test was performed to compare multiple mean groups. Significance between dose/frequency-response curves was determined by two-way repeated ANOVA followed by Bonferroni post hoc analysis. Survival curves were compared via Gehan–Breslow-Wilcoxon Test. Graph Pad Prism V.5.01 software (GraphPad Software, Inc.) was used to generate graphs and perform statistical analysis.

Results

Surgical manipulation of the intestine induces early influx of leukocytes to the ME.

Consistent with previous studies (19), surgical manipulation of the intestine in WT mice led to a significant delay in GI transit (Fig. 1A), accompanied by a massive recruitment of immune cells into the ME during the 24 hours following IM (Fig. S1A). Upon intestinal handling, different immune cells accumulated into the ME with different recruitment patterns/dynamics (Fig. S1B). In line with typical models of sterile inflammation, neutrophils ($CD45^+CD11b^+Ly6G^+CD64^-$) were already detectable in the ME within 1 hour after surgery, peaking at 6 hours and representing 50% of the $CD45^+$ immune cell infiltrate at this time. Subsequently, major recruitment of monocytes/MΦs ($CD45^+CD11b^+Ly6G^-CD64^+$) occurred from 6 hours onwards, outnumbering neutrophils by more than 3-fold at 24 hours after IM (Fig. S1C).

Monocytes recruited to the ME after IM do not induce delay in GI transit.

The recruitment of classical CCR2-monocytes to the sites of tissue inflammation often mediates collateral tissue damage potentially inducing intestinal smooth muscle dysfunction typical of POI. To define the contribution of monocytes in the pathogenesis of POI, we performed IM in mice lacking the CCR2 receptor (*Ccr2*$^{-/-}$) showing defective trafficking of monocytes to the sites of inflammation (20). Of note, lack of CCR2 expression does not alter the typical ME resident MΦ population, with WT and *Ccr2*$^{-/-}$ mice showing similar distribution of $F4/80^+$ cells (Fig. S2A) and comparable number of $MHCII^{lo}$ $Ly6C^-$ MΦs and $MHCII^{hi}$ $Ly6C^-$ MΦs in the naïve ME (Fig. S2B). However, after IM CCR2-deficiency significantly prevented accumulation of monocytes in the ME of *Ccr2*$^{-/-}$ mice compared to WT mice (Fig. 1B). Nevertheless, 24 hours after IM *Ccr2*$^{-/-}$ mice showed delayed GI transit to the same extent as WT mice, excluding a direct effect of monocytes on the development of intestinal dysmotility (Fig. 1A). Moreover, *Ccr2*$^{-/-}$ mice showed similar expression of typical pro-inflammatory cytokines (*tnfa, il6* and *il1a)* and chemokines (*ccl2*, *cxcl1* and *cxcl2)* in the

ME as WT controls 24 hours after IM (Fig. 1C) with the exception of *il1b,* being significantly lower in *Ccr2*$^{-/-}$ mice. Thus, up-regulation of most pro-inflammatory cytokine encoding genes does not depend on monocytes. Taken together, our data indicate that monocytes, although massively recruited to the muscular tissue within 24 hours, are not essential for the initiation of POI.

Functional impairment of gastrointestinal motility in *Ccr2*$^{-/-}$ mice is associated with persistent neuronal impairment after IM.

Upon tissue damage or infection, monocytes are rapidly recruited to the tissue, where they differentiate into mature MΦs, playing an essential role in the resolution of inflammation and tissue repair. Thus, we reasoned that monocytes accumulating in the intestinal ME after IM could differentiate into MΦs being crucial for the resolution of inflammation and recovery. Interestingly, *in vivo* measurements of GI transit after the acute phase of POI (> 24 hours after IM) showed that GI transit delay was significantly prolonged in *Ccr2*$^{-/-}$ mice compared to WT counterparts (Fig. 2A). In detail, while in the WT mice the delay of GI transit mainly recovered 3 days after IM (with few mice recovering at day 5), normalization of GI transit in *Ccr2*$^{-/-}$ mice only started at day 5 with full recover only at day 10 after IM (Fig. 2A). Whereas all WT mice survived IM and recovered GI motility, 25% of *Ccr2*$^{-/-}$ mice failed to recover and died as consequence of prolonged ileus (Fig. 2B).

As GI transit delay in POI mainly depends on reduced functionality of the smooth muscle layer after IM, we determined if the prolonged transit delay observed in *Ccr2*$^{-/-}$ mice was caused by a more severe impairment in neuromuscular function. To this aim, contractility of smooth muscle strips isolated from the small bowel of WT and *Ccr2*$^{-/-}$ mice was recorded at different time points after IM (Fig. 2C-2E) using KCl and the muscarinic agonist carbachol (CCh) to evaluate respectively the Ca^{2+} sensitivity and the receptor-mediated contraction. In line with previous literature (21), IM significantly reduced both receptor-mediated and receptor-independent smooth muscle contractions in WT animals (Fig. S3 and S4). However, contractile responses were significantly smaller in intestinal muscle strips isolated from *Ccr2*$^{-/-}$ mice compared to WT mice 1 day after IM

(Fig. 2C-2D). At day 3 and 5 after IM, myogenic contractions to KCl and CCh were completely recovered both in WT and *Ccr2*$^{-/-}$ muscle strips (Fig. 2C-2D and S3-S4). Furthermore, considering the critical role played by enteric neurons in gastro-intestinal motility, we measured smooth muscle contractions evoked by electrical field stimulation (EFS) to evaluate the impact of IM on the function of enteric nervous system. EFS-induced contractions were reduced in manipulated WT and *Ccr2*$^{-/-}$ animals 1 day after surgery (Fig. S5A), but significantly more pronounced in *Ccr2*$^{-/-}$ mice (Fig. 2E). Contrarily to myogenic responses, EFS-induced contraction remained severely impaired in muscle strips isolated from *Ccr2*$^{-/-}$ mice for 5 days after IM (Fig. 2E and Fig. S5A). Of note, 30% of muscle strips isolated from *Ccr2*$^{-/-}$ mice 3 and 5 days after IM failed to contract to any stimuli suggesting severe alteration of neuromuscular function (data not shown). To evaluate impairment of enteric neurotransmission, EFS-induced contractions were normalized to the receptor-independent KCl-induced contraction of each muscle strip both in WT and *Ccr2*$^{-/-}$ mice at different time points after IM (Fig. S5B). Normalization showed that the "neural component" of EFS-evoked responses was significantly reduced in *Ccr2*$^{-/-}$ compared to WT mice at each time point measured demonstrating a severe dysfunction of enteric neurons after IM in the absence of monocyte recruitment to the ME (Fig. S5B).

In order to assess neural alteration at the morphological level, we used confocal microscopy to dissect the sub-cellular localization of HuC/D in enteric neurons in the myenteric plexus of WT and *Ccr2*$^{-/-}$ mice 5 days after IM (Fig. 3). Our data showed that HuC/D^{+} neurons are comparable in number, volume and neurotransmitters expression of choline acetyltransferase (ChAT) and nitric oxide synthase (nNOS) between the two groups (Fig. S6). However, we detected significantly higher nuclear localization of HuC/D^{+} in enteric neurons of *Ccr2*$^{-/-}$ mice (Fig. 3 and Fig. S7), suggestive of neuronal dysfunction (22;23). Overall, our data showed that neuromuscular function is severely affected in *Ccr2*$^{-/-}$ mice suggesting that monocytes protect neural function during ME inflammation.

Ccr2^{+} monocytes limit inflammation and neutrophil-mediated pathology after IM.

We hypothesized that impaired monocyte trafficking in *Ccr2*$^{-/-}$ mice prevented the switch of the inflammatory process towards resolution, which is orchestrated by monocyte-derived MΦs with regulatory and pro-resolving functions. In fact, local inflammation was prolonged in the ME of *Ccr2*$^{-/-}$ mice, as demonstrated by higher levels of pro-inflammatory cytokines until day 3 after IM (Fig. 4A), and only returning to basal levels at day 5 (data not shown). In addition, the ME of *Ccr2*$^{-/-}$ mice was populated with a higher number of activated neutrophils expressing reactive oxygen species (ROS) as well as IL-6 and TNFα when compared to WT mice (Fig. 4B). In keeping with the implied deregulation of the resolution process, *Ccr2*$^{-/-}$ mice showed increased tissue alterations, as thickening of the intestinal wall and increased deposition of collagen fibres at the level of the ME compared to WT controls (Fig. 4C-3E). Moreover, an increased number of intra-abdominal adhesions were detected 5 days after IM in *Ccr2*$^{-/-}$ mice compared to their WT counterparts (Fig. 4F). These data suggest that monocytes contribute to resolution of inflammation in part by modulating neutrophil influx to the injured ME.

MHCII^{+} monocyte-derived macrophages accumulate in the ME during recovery through CCR2-dependent and independent pathways.

Based upon the evidence that resolution of inflammation and recovery of dysmotility in POI depend on accumulation of monocyte-derived MΦs in the ME, we examined their phenotype and origin at steady state and after surgery in WT and *Ccr2*$^{-/-}$ mice. Of note, the muscularis resident MΦ populations (major population of MHCII^{hi} Ly6C^{-} MΦs and a smaller number of MHCII^{lo} Ly6C^{-} MΦs) of naïve WT and *Ccr2*$^{-/-}$ mice were indistinguishable in shape, number and location (Fig. S2). During the first 24 hours following surgery, neutrophils, classical Ly6C^{hi} monocytes, and Ly6C^{+}MHCII^{+} immature MΦs infiltrated the ME of WT mice (Fig. 5A-4D and Fig. S8). Three days after IM, Ly6C^{hi}MHCII^{-} monocytes were mostly differentiated into Ly6C^{-}MHCII^{lo} and Ly6C^{-}MHCII^{hi} MΦs in equal proportions (Fig. 5E and F). Five days after IM the number of mature MΦs returned to basal levels with a

predominance of MHCII^{hi} MΦs, resembling the steady state situation (Fig. 5A and C). As expected, the recruitment of Ly6C^{hi} monocytes was blunted in *Ccr2*$^{-/-}$ mice at day 1 after IM, associated with a marked reduction of immature and mature MΦs at the later time points compared to their WT counterparts (Fig. 5D-F and Fig. S8). Interestingly, only at day 5 the amount of MHCII^{lo} MΦs in *Ccr2*$^{-/-}$ was comparable to WT mice. This indicated that despite a certain delay, MΦs of the MHCII^{lo} subset can still accumulate in the ME and suggests the presence of CCR2-independent mechanisms of MΦ accumulation (Fig. 5 and Fig. S8).

In order to determine the relative importance of recruited monocytes differentiating *in situ* into MΦs, we first traced the differentiation process via adoptive transfer of Ly6C^{hi} monocytes isolated from UBI-GFP mice into WT mice prior to IM (Fig. 6). GFP^{+} cells were widely detected among the infiltrating monocytes and immature MΦs during the acute phase (day 1) and in both mature MΦ subsets throughout the resolution phase (day 3 and day 5, Fig. 6A and B). Secondly, we assessed the proliferation capacity of monocytes and MΦs in WT naïve ME via BrdU incorporation assay and Ki67 expression. Of note, MHCII^{hi} MΦs in naïve ME incorporated BrdU and expressed Ki67 showing a basal proliferation capacity even at steady state (Fig. 6C and D). After IM, monocytes and immature MΦs showed significant proliferation at day 1, while Ly6C^{-}MHCII^{lo} and Ly6C^{-}MHCII^{hi} MΦs expanded *in situ* mainly at day 3 (Fig. 6C-E). Taken together, these data indicate that MΦ accumulation after IM mainly depends on recruitment and expansion of circulating monocytes and to a minor extent, on the proliferation of resident MΦs. Thus, *Ccr2*$^{-/-}$ mice fail to mount an appropriate and self-limiting inflammatory response, leading to increased tissue damage and prolonged symptoms.

Macrophages acquire pro-resolving features during the recovery phase of POI.

To characterize pro-resolving MΦ features during the recovery phase of POI, we quantified expression levels of genes associated with classical or alternative MΦ activation states in *muscularis* tissue. Within the first few hours after IM (1,5 to 6 hours), pro-inflammatory cytokines *tnfa*, *il6*, *il1b* and *ccl2* were up-regulated (Fig. S9A), while 12 hours after IM typical IL-4-target genes such as *arg1*

and *ym1* were induced (Fig. S9B). Indeed, *il4* itself, which has been implicated in the control of MΦ proliferation during sterile inflammation was highly up-regulated in ME homogenates 12 hours after IM (Fig. S9B). In line, during the resolution phase (day 3 after IM), we detected a significant decrease of inflammatory genes such as *il1b* and an increase in gene expression levels of typical markers of alternative activated MΦs such as *mrc1, stab1* and *ym1* (Fig. 7A). To evaluate which cells express these genes, monocytes, MHCII^{lo} and MHCII^{hi} MΦs were sorted 3 days after IM and expression of pro-inflammatory and pro-resolving genes was evaluated. In detail, high expression of *il1b* and *nos2* were only detectable in monocytic cells, while being significantly lower in mature MΦs. On the contrary, *mrc1*, *arg1*, *stab1* and *ym1* were increased in MΦs compared to monocytes, indicating a differentiation towards a pro-resolving phenotype (Fig. 7B). Of note, expression of these anti-inflammatory markers was higher in the MHCII^{lo} subset (Fig. 7B). Overall, our data showed that MΦs are essential players in resolution of inflammation and restoration of tissue function in POI.

CSF1 drives pro-resolving macrophage differentiation and favours recovery of GI motility.

Based on the above, we hypothesized that favouring monocyte recruitment and their differentiation toward pro-resolving MΦs might represent a valuable therapeutic approach to accelerate recovery of GI function after IM. Thus, considering that the MΦ growth factor CSF1 promotes monocyte production, recruitment, maturation and local MΦ proliferation (24;25), we assessed the effect of CSF1-Fc administration in WT and *Ccr2*$^{-/-}$ mice during the recovery phase after IM (Fig. 8). As previously reported (26), CSF1-Fc treatment increased spleen (Fig. S10A) and liver weight (Fig. S10B) in WT and *Ccr2*$^{-/-}$ mice. Notably, CSF1-Fc treatment restored the accumulation of monocytes and increased MΦ differentiation into the ME of *Ccr2*$^{-/-}$ mice 3 days after IM (Fig. 8A and S11). Of note, CSF1-Fc treatment reduced neutrophil infiltration in the ME of WT and *Ccr2*$^{-/-}$ mice, indicating that monocytes and/or MΦs limited neutrophil entry (Fig. 8A). Consequently, CSF1-Fc-treated mice showed a significantly lower number of ROS-producing neutrophils (Fig. 8B). In addition, CFS1-Fc administration increased the expression of anti-inflammatory and pro-resolving

genes after IM (Fig. S12). Strikingly, with regard to intestinal motility, CSF1-treated *Ccr2*$^{-/-}$ mice recovered GI transit delay 3 days after IM to the same extent as WT mice (Fig. 8C). In line with the beneficial effect of CSF1, adoptive transfer of WT bone marrow into irradiated Ccr*2*$^{-/-}$ mice (WT→ *Ccr2*$^{-/-}$) also induced recovery of GI transit 3 days after IM, which did not differ from that of WT mice reconstituted with WT bone marrow (WT→ WT) (Fig. S13A). Moreover, we observed restored monocyte recruitment to the ME in WT→ *Ccr2*$^{-/-}$ and a significantly lower number of activated neutrophils when compared with non-reconstituted *Ccr2*$^{-/-}$ (Fig. S13 B-D).

Discussion

POI is a clinical condition of iatrogenic origin that occurs after abdominal surgery (1;27). Traditionally, postoperative inhibition of GI transit has been associated with inflammation of the ME and influx of leukocytes (6;9). Although the exact pathogenesis of POI is still not fully understood, prevention of inflammation-associated damage to the intestinal wall is currently considered as a promising therapeutic strategy to shorten postoperative dysmotility (1). Our work revisits the role of incoming monocytes in POI, showing that resolution of ME inflammation and postoperative recovery of GI motility depend upon a population of monocyte-derived MΦs with a pro-resolving phenotype that differentiate *in loco* from $CCR2^+$ inflammatory monocytes.

Leukocytes are recruited to the ME from the circulation a few hours after IM. This process is driven by chemokines secreted *in loco* and by adhesion molecules P-selectin, ICAM-1 and LFA-1 up-regulated on the endothelial surface within few hours after surgery (9;28). Until recently, infiltrating neutrophils and monocytes have been considered the main source of molecules that impair smooth muscle contraction, being responsible for the sustained inhibition of gastrointestinal motility (6;9;10). In line, pre-operative blocking of adhesion molecules such as ICAM-1 and LFA-1, reduced accumulation of leukocytes into the ME, normalized contractile response to the muscarinic agonist bethanecol *in vitro* and ameliorated gastric emptying *in vivo* 24 hours after surgery (6;9;10). However, the specific role played by the different immune cells in the pathogenesis of POI is not fully understood. Several studies reported that once recruited, leukocytes reside up to 7 days in the ME, even beyond the duration of POI, indeed suggesting that they may participate in resolution/recovery phase as well (9;29). Only recently, Stein et al have proposed a dual role for leukocytes recruited to the ME acting as pro-inflammatory cells over the first 24 hours after IM, able to cause tissue damage and functional impairment, but also playing a major role in the resolution process at a later stage (18).

Resolution of inflammation is a coordinated program in which monocyte-derived MΦs play an important role in containing immune-pathology, ceasing neutrophil recruitment, clearing damaged areas and inducing collagen deposition, revascularization, and recovery of tissue function via the secretion of anti-inflammatory cytokines and lipid mediators (14;15;30). In the context of POI, previous studies have already identified some anti-inflammatory mediators such as the immune-modulatory cytokine IL-10 and poly-unsaturated fatty acids (PUFA)-derived pro-resolving mediators involved in resolution of *muscularis* inflammation (18;31;32). Therefore, we hypothesized that, in line with other models of sterile inflammation, monocytes are essential for the resolution ME inflammation in POI.

Hence, in order to assess the role of incoming monocytes in POI, we employed intestinal manipulation in *Ccr2*$^{-/-}$ mice, lacking the CCR2 receptor and therefore unable to recruit CCR2-monocytes referred to as pro-inflammatory (20). Currently, murine intestinal manipulation of the intestine is widely used as a preclinical model of POI. This model recapitulates important clinical phenomena of the POI seen in surgical patients such as inflammatory response in the muscle layer of the intestine and delay of GI transit. Interestingly, functional and inflammatory parameters measured 24 hours after surgery in *Ccr2*$^{-/-}$ mice did not differ from those of control mice showing that preventing monocyte influx does not impact on the development of POI. Conversely, we observed a significant delay in the recovery of GI motility in *Ccr2*$^{-/-}$ mice, accompanied by more severe alterations of the neuromuscular function and increased inflammation. In fact, most of the *Ccr2*$^{-/-}$ mice only recovered 10 days after IM and in some cases these mice even succumb before complete recovery. In vitro, the effects of IM on muscle contractions were significantly potentiated, especially as EFS-induced contractions remained altered for several days after IM. Interestingly, prolonged neural dysfunction in *Ccr2*$^{-/-}$ mice was mirrored by typical signs of neuronal distress, as evidenced by the translocation of HuC/D to the nuclei of enteric neurons (22;23). Overall, neuromuscular alterations in *Ccr2*$^{-/-}$ mice were associated with an increased and long lasting expression of pro-inflammatory cytokines in the ME, resulting in augmented deposition of collagen

fibers and intra-abdominal adhesions. Considering the larger amount of IL-6^{+} and ROS^{+} neutrophils found in the ME of *Ccr2*$^{-/-}$ mice, it seemed likely that in the absence of monocyte-derived MΦs neutrophil clearance is impaired and the entire resolution process is disrupted, leading to a delayed functional recovery.

Furthermore, as for other models of sterile inflammation after acute injury, we demonstrated that also in POI inflammatory monocytes recruited to the ME acquired a pro-resolving phenotype. We showed indeed that IL-4 itself, and IL-4 target genes were expressed in the ME at very early time points after IM. In addition, anti-inflammatory genes *arg1*, *ym1* and *il10* and genes encoding for pro-resolving mediators such as *mrc1, stab1 and ym1* were found up-regulated at a later stage, mainly 3 days after IM. Cell sorting experiments confirmed the expression of these markers mainly in MHCII^{+} mature MΦs isolated from the ME 3 days after surgery. Of note, beside alternative activation of monocyte-derived MΦs, expansion of resident MΦs has been shown to be an important mechanism in sterile inflammatory models (33-37). Interestingly, we found that MΦs held proliferative activity and expanded *in situ*. Thus, we speculate that *muscularis* resident MΦs proliferate after surgical trauma. This would explain why MHCII^{lo} MΦs populated the injured ME of *Ccr2*$^{-/-}$ mice, albeit with significant delay compared to WT.

In conclusion, the results presented here suggest that monocyte recruitment is dispensable for the onset of POI. Hence, we favor the view that mainly ME resident MΦs activated during abdominal surgery release cytokines, prostaglandins and NO leading to impairment of neuromuscular function and ileus, and at the same time triggering the influx of inflammatory cells, mainly monocytes and neutrophils (38;39). Monocytes, entering the muscularis in a CCR2-dependent manner, will differentiate into MΦs resolving the inflammation and restoring intestinal function. Eventually, we showed that monocyte migration and differentiation to pro-resolving MΦs can be enhanced via CSF1 administration. Among the growth factors regulating monocyte/MΦ biology, CSF1 is an essential regulator of MΦ homeostasis (24), involved in monocyte entry into the

circulation (25;40) , monocyte/MΦ proliferation and polarization towards an immune-suppressive and tissue-repair phenotype (41). CSF1 treatment was in fact able to overcome the monocyte deficiency in *Ccr2*$^{-/-}$ mice, and thus promote repair and recovery after IM. In line, CSF1 has been shown to promote tissue recovery in models of ischemic damage to the kidneys (42), heart (43) and after partial hepatectomy (44) due to the presence of pro-resolving MΦ. In this context, CSF1-Fc fusion protein, with increased half-life and stability compared to recombinant CSF1, holds potential as a novel approach to accelerate recovery of POI (45).

Overall, from a therapeutic point of view, our findings imply that future therapies for POI should preferentially enhance tissue repair by promoting maturation of monocytes into MΦs with pro-resolving capacity rather than blocking recruitment of monocytes to the tissue.

Acknowledgments

The authors would like to thank I. Appeltans, J. Vandewalle and R. De Keyser (Translational Research Center for Gastrointestinal Disorders, KU Leuven, Belgium) for their excellent technical assistance.

Footnotes

Contributors

GF: acquisition of data, analysis and interpretation of data; drafting of the manuscript; PJG-P, MDG, EL, EM, FDE, MS, NS, YE, ZL, KS and DL: acquisition of data, analysis and interpretation of data; JVG and DAH: provided essential material and critical revision of the manuscript; GM and GEB: study concept and design; interpretation of data; obtained funding.

Grant support

This work was supported by grants from the Research Foundation – Flanders (FWO) (Odysseus program (G.0905.07) and FWO grant (G.0566.12N) to G.E.B, by a FWO PhD fellowship (to M.DG) and by FWO postdoctoral research fellowships (to G.M. and P.J.G).

Competing interests

The authors declare no financial, professional or personal conflicts relevant to the manuscript.

Ethics approval

Animal Care and Animal Experiments Committee of the University of Leuven (Leuven, Belgium)

Figure legends.

Figure 1. **Monocyte depletion does not prevent the development of POI.** WT and *Ccr2*$^{-/-}$ mice were subjected to IM and GI transit evaluated after 24 hours. (A) Dots represent geometric centre (GC) values of fluorescence distribution through the intestinal segments 90 minutes after oral administration of dextran-FITC in individual mice, mean ± SEM is also shown. WT and *Ccr2*$^{-/-}$ data sets of each condition were compared with their relative naïve control via unpaired t-test (*** $P <$ 0.0001). (B) Frequency and absolute numbers of $CD45^{+}CD11b^{+}Ly6G^{-}Ly6C^{hi}MHCII^{-}$ monocytes in WT (white bars) and *Ccr2*$^{-/-}$ mice (black bars) before and 1 day after IM. Data are shown as mean ± SEM. Statistical significance between WT and *Ccr2*$^{-/-}$ data sets was determined via unpaired t-test (*** $P <$ 0.0001 and ns= not significant). (C) Fold changes over naïve mic e of cytokine mRNA levels 1 day after IM are shown as mean ± SEM. Data sets were compared via unpaired t-test (* $P < 0.05$, ns= not significant). Data are representative of 3 independent experiments.

Figure 2. Preventing monocyte recruitment reduces smooth muscle contraction, GI motility *in vivo* and affects survival after intestinal manipulation. WT and *Ccr2*$^{-/-}$ mice were subjected to IM and GI transit was assessed 1, 3, 5 and 10 days after IM. (A) Graph represents GC values mean ± SEM from WT and *Ccr2*$^{-/-}$ mice at indicated time point after IM. WT and *Ccr2*$^{-/-}$ data sets were compared with two-way ANOVA test followed by Bonferroni correction (** $P < 0.001$, *** $P < 0.0001$ and ns= not significant). Data are representative of 3 independent experiments. (B) Percentage survival rate shown as a Kaplan-Meier survival curve. Survival curves were compared via Gehan-Breslow-Wilcoxon test (* $P < 0.05$). (C-E) Ileal smooth muscle strips from WT and *Ccr2*$^{-/-}$ mice at 1, 3 and 5 days after IM were stimulated *in vitro* to assess myogenic and neurogenic contractions. Each data set includes 6 mice. Data are representative of 3 independent experiments. (C) Mean values (in mN/mm^2) ± SEM of contractile responses to KCl (60 mM). WT and *Ccr2*$^{-/-}$ data sets were compared at each time point via unpaired t-test (** $P < 0.001$ and ns= not significant). (D) Mean values (in mN/mm^2) ± SEM of contractile responses to increasing concentrations of carbachol (CCh). WT and

Ccr2$^{-/-}$ dose response curves were compared via two-way ANOVA test followed by Bonferroni correction (** P < 0.001, ns= not significant). (E) Mean values (in mN/mm^2) ± SEM of contractile responses to EFS at increasing frequencies. WT and *Ccr2*$^{-/-}$ frequency- response curves were compared via two-way ANOVA test followed by Bonferroni correction (* P < 0.05 and ** P < 0.001).

Figure 3. Lack of CCR2-monocytes induces enteric neuronal alteration after intestinal manipulation. WT and *Ccr2*$^{-/-}$ mice were subjected to IM and the myenteric plexus and enteric neurons analysed 5 days after IM. (A) Representative confocal images of whole mount ME preparations from WT and *Ccr2*$^{-/-}$ mice. Neuronal cell bodies are identified via HuC/D (red), the interganglionic connections via neurofilament (NF200; green) and nuclei using DAPI (blue), scale bar is 20µm. (B) Volume of individual HuC/D$^+$ enteric neurons in WT and *Ccr2*$^{-/-}$ mice 5 days after IM are represented, mean are shown for both groups as white line. (C) Fluorescent intensity of HuC/D in individual enteric neuronal nuclei is shown. (D) Percentage of HuC/D fluorescent intensity in the nucleus of individual enteric neuronal nuclei versus the total cellular HuC/D is shown, median are shown for both groups as white line. WT and *Ccr2*$^{-/-}$ data sets were compared via unpaired t-test (*** *P* < 0.001, ns= not significant).

Figure 4. Persistent inflammation, neutrophil-mediated pathology and increased fibrosis in *Ccr2*$^{-/-}$ mice after IM. WT and *Ccr2*$^{-/-}$ mice were subjected to IM and inflammatory parameters were analyzed at day 3. (A) Fold changes over naïve mice of cytokine mRNA levels 3 days after IM are shown as mean ± SEM. Data sets were compared via unpaired t-test (* *P* < 0.05, ** *P* < 0.001, ns= not significant). (B) Absolute numbers of CD11b$^+$Ly6G$^+$ neutrophils, ROS$^+$ neutrophils, IL-6$^+$ neutrophils and TNFα$^+$ neutrophils isolated 1 and 3 days after IM. WT and *Ccr2*$^{-/-}$ were compared at both time points via unpaired t-test (*** *P* < 0.0001), data are representative of 3 independent experiments. (C) Representative images of Masson's trichrome staining in small intestine cross sections of naïve WT and *Ccr2*$^{-/-}$ mice and at 5 days after IM. (D) Measurements of *muscularis* thickness are shown as mean ± SEM for naïve mice and 5 days after IM. Data sets were compared

with naïve via unpaired t-test (* $P < 0.05$). WT and *Ccr2*$^{-/-}$ data sets were compared at both time points via unpaired t-test (* $P < 0.05$ and ns= not significant). (E) Percentages of collagen in small intestine cross sections are shown as mean values ± SEM. WT and *Ccr2*$^{-/-}$ mice were compared at both time points via unpaired t-test (* $P < 0.05$, ns= not significant). (F) Peritoneal adhesions were scored in WT and *Ccr2*$^{-/-}$ mice before and 5 days after IM. WT and *Ccr2*$^{-/-}$ data sets were compared at both time points via unpaired t-test (* $P < 0.05$, ns= not significant).

Figure 5. Mature macrophages accumulate into the *muscularis externa* during recovery. Immune cells isolated from the ME of naïve WT and *Ccr2*$^{-/-}$ mice and 1, 3 and 5 days after IM were analyzed via flow cytometry. (A) Representative dot plot showing CD11b^{+}Ly6G^{+} neutrophils and CD11b^{+}Ly6G^{-} cells gated on the CD45^{+} population. Ly6C^{hi}MHCII^{-} monocytes, Ly6C^{+}MHCII^{+} immature MΦs, and Ly6C^{-}MHCII^{lo} and Ly6C^{-}MHCII^{hi} MΦs were gated on the CD11b^{+}Ly6G^{-} population. Absolute numbers of neutrophils (B), Ly6C^{hi}MHCII^{-} monocytes (C), Ly6C^{+}MHCII^{+} immature MΦs (D) and Ly6C^{-}MHCII^{lo} (E), and Ly6C^{-}MHCII^{hi} MΦs (F), in WT (white bars) and *Ccr2*$^{-/-}$ mice (black bars). Data are shown as mean ± SEM. Statistical significance between WT and *Ccr2*$^{-/-}$ data sets was determined via unpaired t-test (* $P < 0.05$, ** $P < 0.001$, *** $P < 0.0001$ and ns= not significant) data are representative of 3 independent experiments.

Figure 6. Mature macrophages originate from CCR2^{+} monocytes and from proliferating resident macrophages. Ly6C^{hi} monocytes were isolated from UBI-GFP reporter mice and injected i.v. into WT mice 1 hr before IM to trace monocyte differentiation *in situ*. (A) Dot plot representing GFP^{+} cells in the ME of naïve mice and at 1, 3 and 5 days after IM. (B) Frequencies of Ly6C^{hi}MHCII^{-} monocytes, Ly6C^{+}MHCII^{+} immature MΦs, Ly6C^{-}MHCII^{lo} and Ly6C^{-}MHCII^{hi} MΦs within the GFP^{+} cells. Data are shown as mean ± SEM. Data are representative of 2 independent experiments. (C) A pulse of BrdU was given to naïve WT mice and at 1, 3 and 5 days after IM. Proliferation rate of immune cells isolated from ME was assessed via FACS analysis. (C) Absolute numbers of BrdU positive Ly6C^{hi}MHCII^{-} monocytes, Ly6C^{+}MHCII^{+} immature MΦs and Ly6C^{-}MHCII^{lo} or Ly6C^{-}MHCII^{hi} MΦs. (D) Ki67 staining

was assessed in naïve WT mice and at 1, 3 and 5 days after IM. Proliferation rate of immune cells isolated from ME was assessed via FACS analysis. (D) Absolute numbers of Ki67 positive Ly6C^{hi}MHCII^{-} monocytes, Ly6C^{+}MHCII^{+} immature MΦs and Ly6C^{-}MHCII^{lo} or Ly6C^{-}MHCII^{hi} MΦs. Each data set included 6 mice. Data are shown as mean ± SEM representative of 2 independent experiments. All data sets were compared to data in naïve mice via one-way ANOVA followed by Dunnett's Multiple Comparison Test (* $P < 0.05$, ** $P < 0.001$ and *** $P < 0.0001$).

Figure 7. Monocyte-derived macrophages hold a pro-resolving phenotype. Gene expression levels of pro-inflammatory and pro-resolving markers were measured in homogenates of ME of WT mice at different time points after IM (A), and in monocytes and MΦs isolated via cell sorting from the ME of WT mice 3 days after IM (B). In A data are expressed as fold change mean values ± SEM over naïve mice. In B mRNA levels (mean values ± SEM) in sorted monocytes and MΦs expressed as relative expression of the gene of interest over the expression of the reference gene *rpl32*. Data are representative of 3 independent experiments.

Figure 8. CSF1 drives pro-resolving macrophage differentiation and favours recovery of GI motility. WT and Ccr2$^{-/-}$ mice undergoing IM were treated with either (0.75 µg/g) CSF1-Fc or saline. Functional and inflammatory parameters were assessed 3 days after IM. (A) Absolute numbers of Ly6C^{hi}MHCII^{-} monocytes, Ly6C^{+}MHCII^{+} immature MΦs, Ly6C^{-}MHCII^{lo} and Ly6C^{-}MHCII^{hi} MΦs in WT and *Ccr2*$^{-/-}$ mice. Statistical significance between CSF1-Fc and saline-treated data sets was determined via unpaired t-test (* $P < 0.05$, ** $P < 0.001$, *** $P < 0.0001$ and ns= not significant). (B) Absolute numbers of ROS^{+} neutrophils. Statistical significance between CSF1-Fc and saline-treated data sets was determined via unpaired t-test (** $P < 0.001$). (C) Dots represent GC values from individual mice; mean ± SEM are also shown. Statistical significance between CSF1-Fc and saline-treated data sets was determined via unpaired t-test (* $P < 0.05$).

Reference List

(1) Boeckxstaens GE, de Jonge WJ. Neuroimmune mechanisms in postoperative ileus. *Gut* 2009;**58**(9):1300-11.

(2) Asgeirsson T, El-Badawi KI, Mahmood A *et al*. Postoperative ileus: it costs more than you expect. *Journal of the American College of Surgeons* 2010;**210**(2):228-31.

(3) Mikkelsen HB, Thuneberg L, Rumessen JJ *et al*. Macrophage-like cells in the muscularis externa of mouse small intestine. *Anat Rec* 1985;**213**(1):77-86.

(4) Kalff JC, Turler A, Schwarz NT *et al*. Intra-abdominal activation of a local inflammatory response within the human muscularis externa during laparotomy. *Ann Surg* 2003;**237**(3):301-15.

(5) Muller PA, Koscso B, Rajani GM *et al*. Crosstalk between muscularis macrophages and enteric neurons regulates gastrointestinal motility. *Cell* 2014;**158**(2):300-13.

(6) de Jonge WJ, van den Wijngaard RM, The FO *et al*. Postoperative ileus is maintained by intestinal immune infiltrates that activate inhibitory neural pathways in mice. *Gastroenterology* 2003;**125**(4):1137-47.

(7) Wehner S, Behrendt FF, Lyutenski BN *et al*. Inhibition of macrophage function prevents intestinal inflammation and postoperative ileus in rodents. *Gut* 2007;**56**(2):176-85.

(8) Matteoli G, Gomez-Pinilla PJ, Nemethova A *et al*. A distinct vagal anti-inflammatory pathway modulates intestinal muscularis resident macrophages independent of the spleen. *Gut* 2014;**63**(6):938-48.

(9) Kalff JC, Carlos TM, Schraut WH *et al*. Surgically induced leukocytic infiltrates within the rat intestinal muscularis mediate postoperative ileus. *Gastroenterology* 1999;**117**(2):378-87.

(10) The FO, de Jonge WJ, Bennink RJ *et al*. The ICAM-1 antisense oligonucleotide ISIS-3082 prevents the development of postoperative ileus in mice. *Br J Pharmacol* 2005;**146**(2):252-8.

(11) Shechter R, London A, Varol C *et al*. Infiltrating blood-derived macrophages are vital cells playing an anti-inflammatory role in recovery from spinal cord injury in mice. *PLoS Med* 2009;**6**(7):e1000113.

(12) Zigmond E, Samia-Grinberg S, Pasmanik-Chor M *et al*. Infiltrating monocyte-derived macrophages and resident kupffer cells display different ontogeny and functions in acute liver injury. *J Immunol* 2014;**193**(1):344-53.

(13) Nahrendorf M, Pittet MJ, Swirski FK. Monocytes: protagonists of infarct inflammation and repair after myocardial infarction. *Circulation* 2010;**121**(22):2437-45.

(14) Grainger JR, Wohlfert EA, Fuss IJ *et al*. Inflammatory monocytes regulate pathologic responses to commensals during acute gastrointestinal infection. *Nat Med* 2013;**19**(6):713-21.

(15) Serhan CN, Savill J. Resolution of inflammation: the beginning programs the end. *Nat Immunol* 2005;**6**(12):1191-7.

(16) Stoffels B, Schmidt J, Nakao A *et al*. Role of interleukin 10 in murine postoperative ileus. *Gut* 2009;**58**(5):648-60.

(17) Wehner S, Meder K, Vilz TO *et al*. Preoperative short-term parenteral administration of polyunsaturated fatty acids ameliorates intestinal inflammation and postoperative ileus in rodents. *Langenbecks Arch Surg* 2012;**397**(2):307-15.

(18) Stein K, Stoffels M, Lysson M *et al*. A role for 12/15-lipoxygenase-derived proresolving mediators in postoperative ileus: protectin DX-regulated neutrophil extravasation. *J Leukoc Biol* 2016;**99**(2):231-9.

(19) van Bree SH, Nemethova A, van Bovenkamp FS *et al*. Novel method for studying postoperative ileus in mice. *Int J Physiol Pathophysiol Pharmacol* 2012;**4**(4):219-27.

(20) Kurihara T, Warr G, Loy J *et al*. Defects in macrophage recruitment and host defense in mice lacking the CCR2 chemokine receptor. *J Exp Med* 1997;**186**(10):1757-62.

(21) Farro G, Gomez-Pinilla PJ, Di GM *et al*. Smooth muscle and neural dysfunction contribute to different phases of murine postoperative ileus. *Neurogastroenterol Motil* 2016;**28**(6):934-47.

(22) Cirillo C, Bessissow T, Desmet AS *et al*. Evidence for neuronal and structural changes in submucous ganglia of patients with functional dyspepsia. *Am J Gastroenterol* 2015;**110**(8):1205-15.

(23) Desmet AS, Cirillo C, Vanden Berghe P. Distinct subcellular localization of the neuronal marker HuC/D reveals hypoxia-induced damage in enteric neurons. *Neurogastroenterol Motil* 2014;**26**(8):1131-43.

(24) Stanley ER, Cifone M, Heard PM *et al*. Factors regulating macrophage production and growth: identity of colony-stimulating factor and macrophage growth factor. *J Exp Med* 1976;**143**(3):631-47.

(25) Hume DA, Pavli P, Donahue RE *et al*. The effect of human recombinant macrophage colony-stimulating factor (CSF-1) on the murine mononuclear phagocyte system in vivo. *J Immunol* 1988;**141**(10):3405-9.

(26) Gow DJ, Sauter KA, Pridans C *et al*. Characterisation of a novel Fc conjugate of macrophage colony-stimulating factor. *Mol Ther* 2014;**22**(9):1580-92.

(27) Bauer AJ, Boeckxstaens GE. Mechanisms of postoperative ileus. *Neurogastroenterol Motil* 2004;**16 Suppl 2**:54-60.

(28) Kalff JC, Schraut WH, Simmons RL *et al*. Surgical manipulation of the gut elicits an intestinal muscularis inflammatory response resulting in postsurgical ileus. *Ann Surg* 1998;**228**(5):652-63.

(29) Wehner S, Vilz TO, Stoffels B *et al*. Immune mediators of postoperative ileus. *Langenbecks Arch Surg* 2012;**397**(4):591-601.

(30) Serhan CN, Chiang N, Dalli J *et al*. Lipid mediators in the resolution of inflammation. *Cold Spring Harb Perspect Biol* 2015;**7**(2):a016311.

(31) Stoffels B, Schmidt J, Nakao A *et al*. Role of interleukin 10 in murine postoperative ileus. *Gut* 2009;**58**(5):648-60.

(32) Wehner S, Meder K, Vilz TO *et al*. Preoperative short-term parenteral administration of polyunsaturated fatty acids ameliorates intestinal inflammation and postoperative ileus in rodents. *Langenbecks Arch Surg* 2012;**397**(2):307-15.

(33) Little MC, Hurst RJ, Else KJ. Dynamic changes in macrophage activation and proliferation during the development and resolution of intestinal inflammation. *J Immunol* 2014;**193**(9):4684-95.

(34) Van GN, Van OE, Leuckx G *et al*. Macrophage dynamics are regulated by local macrophage proliferation and monocyte recruitment in injured pancreas. *Eur J Immunol* 2015;**45**(5):1482-93.

(35) Davies LC, Rosas M, Jenkins SJ *et al*. Distinct bone marrow-derived and tissue-resident macrophage lineages proliferate at key stages during inflammation. *Nat Commun* 2013;**4**:1886.

(36) Jenkins SJ, Ruckerl D, Thomas GD *et al*. IL-4 directly signals tissue-resident macrophages to proliferate beyond homeostatic levels controlled by CSF-1. *J Exp Med* 2013;**210**(11):2477-91.

(37) Jenkins SJ, Ruckerl D, Cook PC *et al*. Local macrophage proliferation, rather than recruitment from the blood, is a signature of TH2 inflammation. *Science* 2011;**332**(6035):1284-8.

(38) Kalff JC, Schraut WH, Billiar TR *et al*. Role of inducible nitric oxide synthase in postoperative intestinal smooth muscle dysfunction in rodents. *Gastroenterology* 2000;**118**(2):316-27.

(39) Hori M, Kita M, Torihashi S *et al*. Upregulation of iNOS by COX-2 in muscularis resident macrophage of rat intestine stimulated with LPS. *Am J Physiol Gastrointest Liver Physiol* 2001;**280**(5):G930-G938.

(40) Van OE, Stijlemans B, Heymann F *et al*. M-CSF and GM-CSF Receptor Signaling Differentially Regulate Monocyte Maturation and Macrophage Polarization in the Tumor Microenvironment. *Cancer Res* 2016;**76**(1):35-42.

(41) Martinez FO, Gordon S, Locati M *et al*. Transcriptional profiling of the human monocyte-to-macrophage differentiation and polarization: new molecules and patterns of gene expression. *J Immunol* 2006;**177**(10):7303-11.

(42) Alikhan MA, Jones CV, Williams TM *et al*. Colony-stimulating factor-1 promotes kidney growth and repair via alteration of macrophage responses. *Am J Pathol* 2011;**179**(3):1243-56.

(43) Okazaki T, Ebihara S, Asada M *et al*. Macrophage colony-stimulating factor improves cardiac function after ischemic injury by inducing vascular endothelial growth factor production and survival of cardiomyocytes. *Am J Pathol* 2007;**171**(4):1093-103.

(44) Stutchfield BM, Antoine DJ, Mackinnon AC *et al*. CSF1 Restores Innate Immunity After Liver Injury in Mice and Serum Levels Indicate Outcomes of Patients With Acute Liver Failure. *Gastroenterology* 2015;**149**(7):1896-909.

(45) Hume DA, MacDonald KP. Therapeutic applications of macrophage colony-stimulating factor-1 (CSF-1) and antagonists of CSF-1 receptor (CSF-1R) signaling. *Blood* 2012;**119**(8):1810-20.